# PURIFICATION AND PARTIAL CHARACTERIZATION OF GLUTATHIONE S-TRANSFERASES FROM *Pseudomonas* sp. UW4

CHRISTINA KONG WEN HUI

FACULTY OF SCIENCE
UNIVERSITY OF MALAYA
KUALA LUMPUR

2019

# PURIFICATION AND PARTIAL CHARACTERIZATION OF GLUTATHIONE S-TRANSFERASES FROM *Pseudomonas* sp. UW4

**CHRISTINA KONG WEN HUI**

**DISSERTATION SUBMITTED IN FULFILMENT OF THE REQUIREMENTS FOR THE DEGREE OF MASTER OF SCIENCE**

**INSTITUTE OF BIOLOGICAL SCIENCES**
**FACULTY OF SCIENCE**
**UNIVERSITY OF MALAYA**
**KUALA LUMPUR**

**2019**

**UNIVERSITY MALAYA**

**ORIGINAL LITERARY WORK DECLARATION**

Name of candidate :**CHRISTINA KONG WEN HUI**

Registration/Matric no: **SGR 140072**

Name of Degree : **MASTER OF SCIENCE**

Title of Project Paper/Research Project/ Dissertation/ Thesis ("this Work"):

**PURIFICATION AND PARTIAL CHARACTERIZATION OF GLUTATHIONE S-TRANSFERASES FROM *Pseudomonas* sp. UW4**

Field of Study:

**MICROBIOCHEMISTRY**

I do solemnly and sincerely declare that

(1) I am the sole author/ writer of this Work;
(2) This Work is original;
(3) Any use of any work in which copyright exists was done by way of fair dealing and for permitted purposes and any except or extract from, or reference to or reproduction of any copyright work has been disclosed expressly and sufficiently and the title of the Work and its authorship have been acknowledged in this Work;
(4) I do not have any actual knowledge nor do I ought reasonably to know that the making of this Work constitutes an infringement of any copyright work;
(5) I hereby assign all and every rights in the copyright to this Work to the University of Malaya ("UM"), who here forth shall be owner of the copyright to this Work and that any reproduction or use in any form or by any means whatsoever is prohibited without the written consent UM having been first had and obtained;
(6) I am fully aware that if in the course of making this Work I have infringed any copyright whether intentionally or otherwise, I may be subject to legal action or any other action as may be determined by UM.

Candidature's Signature Date

Subscribed and solemnly declared before,

Witness's Signature Date

Name :
Designation :

**PURIFICATION AND PARTIAL CHARACTERIZATION OF GLUTATHIONE S-TRANSFERASES FROM *Pseudomonas* sp. UW4**

## ABSTRACT

Glutathione transferases (GSTs) obtained from University of Waterloo, Canada, were purified from *Pseudomonas* sp. UW4, by glutathione-affinity chromatography, identified through bioinformatic analysis and their substrate specificities were investigated. SDS-polyacrylamide gel electrophoresis revealed that the GST purified using Sulfobromophthalein-glutahione (BSP) affinity column resolved into a single band with low molecular weight (MW) of 17 kDa. Isoselectrofocusing showed it exists in single band with pI value of 6.1. Purified GST was reactive towards ethacrynic acid, 1-chloro-2,4-dinitrobenzene, cumene hydroxide and hydrogen peroxide, but no detectable activity with trans-2-octenal, hepta-2,4-dienal and trans-4-phenyl-3-butene-2-one. This demonstrated that putative GST possessed peroxidase activity but is not involved in lipid peroxidation. The purified GST suggested to be similar to PputUW4_00801 (putative glutathione S-transferase) of *Pseudomonas* sp. UW4.

**Keywords**: Purification, glutathione-s-transferase, Sulfobromophthalein-glutahione, affinity column, *Pseudomonas* sp. UW4

**PENULENAN DAN PENGECAMAN SEPARA GLUTATHIONE S-TRANSFERES DARIPADA *Pseudomonas* sp. UW4**

## ABSTRAK

*Glutathione transferes* (GSTs) yang diperoleh daripada Universiti Waterloo, Kanada, telah ditulenkan daripada *Pseudomona*s sp. UW4, menggunakan kromatografi affiniti-glutathione, diidentifikasi melalui analisis bioinformatik dan spesifikasi subtraknya telah dikaji. Gel elektroforesis SDS-polyacrylamide mendapati GST yang ditulenkan menggunakan kolum affiniti glutathione-sulfobromophthalein (BSP) membawa kepada kemunculan satu jalur protein dengan berat molekul yang rendah iaitu 17 kDa. Titik isoelektrik menunjukkan bahawa ia muncul dalam sejenis isoform dengan pI 6.1. GST yang telah ditulenkan adalah reaktif terhadap asid etakrinik, 1-kloro-2,4-dinitrobenzena, kumena hidroksida dan hidrogen peroksida, tetapi tidak menunjukkan sebarang aktiviti terhadap trans-2-oktenal, hepta-2,4-dienal dan trans-4-phenyl-3-butena-2-one. Ini menunjukkan bahawa GST putatif mempunyai aktiviti peroksida tetapi tidak terlibat dalam pengoksidaan lipid. GST yang ditulenkan dicadangkan menyerupai PputUW4_00801 (glutathione S-transferase putatif) bagi *Pseudomonas* sp. UW4.

**Kata kunci**: Penulenan, glutathione-s-transferase, Sulfobromophthalein-glutahione, affiniti column, *Pseudomonas* sp. UW4

## ACKNOWLEDGEMENTS

I would like also to express my heartfelt gratitude and indebtedness to my project supervisor, Associate Prof. Dr. Zazali Alias, who gave me the opportunity to conduct this research, for his continuous guidance, patience, constructive criticism, invaluable advice and unreserved assistance throughout out this project.

I am also indebted to my co-supervisor, Prof Irene Tan Kit Ping for her invaluable guidance and encouragement which kept me in a right track Not forgetting, the memories I shared with my lab mates especially Ema, Nasiru Abdullah, Dayyabu Shehu, Abiramy, Juwaini bin Mohd Yusoff. I would like to take this opportunity to express my gratitude over their continuous support and helping hand throughout my quest for success.

I also would like to thank my family for all the financial support and encouragement, contribution, hope and prayers for me to endure the obstacles that I have been through. The hope of obtaining a higher degree is the best reward to my parents.

## TABLE OF CONTENTS

## LIST OF FIGURES

## LIST OF TABLES

## LIST OF SYMBOLS AND ABBREVIATIONS

| | |
|---|---|
| d | : Diameter of cuvette (cm) |
| ε | : $Lmmol^{-1}cm^{-1}$ |
| *Km* | : Substrate concentration at half the maximum enzyme velocity |
| PBO | : Trans-4-phenyl-3-butene-2-one |
| t | : time in minutes |
| [V] | : Velocity |
| V | : Assay volume in L |
| v | : Sample volume; |
| $V_{max}$ | : Maximum initial rate of enzyme |
| [protein] | : Concentration of protein (mg/l) |
| [S] | : Substrate concentration |
| ΔAbs | : Change in absorbance |
| 2D | : 2 dimensional |
| 3D | : 3 dimensional |
| Abs | : Absorbance |
| ACC | : 1-aminocyclopropane-1-carboxylate |
| APS | : Ammonium persulphate |
| ATP | : Adenosine triphosphate |
| Bp | : Base pair |
| BSP | : Sulfobromopthalein |
| CBB | : Colloidal brilliant blue |
| CDNB | : 1-chloro-2,4-dinitrobenzene |
| cGST | : Cytosolic GST |
| CHAPS | : 3-[(3-cholamidopropyl)dimethylammonio]-1-propanesulfonate |
| CHCA | : α-Cyano-4-hydroxycinnamic acid |

DCNB : 1,2-dichloro-4-nitrobenzene

DEAE : Diethylaminoethyl

EA : Ethacrynic acid

EB : Equilibration buffer

EDTA : Ethylenediaminetetraacetic acid

Fos A : Fosfomycin A

Fos B : Fosfomycin B

Fos C : Fosfomycin C

Fos X : Fosfomycin X

FPLC : Fast protein liquid chromatography

GSH : Glutathione tripeptide

GSSR : Glutathione reductase

GST : Glutathione S-transferases

hGSTK1 : Human GST kappa-1

hGSTP : Human GST pi

IEF : Isoelectric focusing

kDa : Kilodaltons

MALDI-TOF : Matrix assisted laser desorption/ionization-time of flight

MAPEG : Membrane-associated proteins in eicosanoid and glutathione metabolism

$Mn^{2+}$ : Manganese ion +2

NaCl : Sodium chloride

NADH : Nicotinamide adenine dinucleotide

NADPH : Nicotinamide adenine dinucleotide phosphate

NBC : p-nitrobenzyl chloride

NCBI : *National center for biotechnology information*

PCR : Polymerase chain reaction

PDB : Protein Data Bank

PG : Prostaglandins

PmGST : *Proteus mirabilis* GST

PTU : Phenylthiourea

ROS : Reactive oxygen species

rRNA : ribosomal ribonucleic acid

SDS : sodium dodecyl sulfate

SDS-PAGE : sodium dodecyl sulfate polyacrylamide gel electrophoresis

SeGST : *Synechococcus elongatus* PCC 6301 GSTs

Ser : Serine

$T_20$ : Trans-2-octenal

TCHQ : tetrachlorohydroquinone

TeGST : *Thermosynechococcus elongatus* BP-1 GST

TEMED : Tetramethylethylenediamine

TLC : Thin layer chromatography

Tris HCl : Tris(hydroxymethyl)aminomethane hydrochloride

## LIST OF APPENDICES

## LIST OF FORMULAS

# CHAPTER 1: INTRODUCTION

Bacterial GSTs have important roles in chemical transformations and detoxification due to their sequence variability and functional versatility. Bacterial GSTs involve in biodegradation of harmful chemicals, protection against both oxidative and chemical stresses, cellular protection from reactive oxygen species, degradation of certain monocyclic aromatic chemical, and antimicrobial drug resistance have proven that bacterial GSTs in biodegradation and thus bioremediation (Allocati *et al.*, 2009).

*Pseudomonas* sp. UW4 is plant growth-promoting bacteria (PGPB), was obtained from University of Waterloo, Ontario, Canada. It was originated from the rhizosphere of common reeds found near the campus which enhance plant growth in different environmental stresses. They able to resist and growth under condition when there is flood, presence of heavy metals, high concentrations of salt, cold, drought and phytopathogens (Duan *et al.*, 2013). Hence, it would be thought-provoking to study about the contribution of GSTs towards environmental stresses. This project serves as a preliminary study of identifying putative GSTs of *Pseudomonas* sp. UW4 through bioinformatic analysis, purifying expressed GSTs from *Pseudomonas* sp. UW4 and characterizing the purified GSTs.

## 1.1 Objectives

Two objectives of this study are as stated below:

- To purify expressed GSTs from *Pseudomonas* sp.UW4
- To biochemically and bioinformatically characterize the purified GSTs from *Pseudomonas* sp.UW4

# CHAPTER 2: LITERATURE REVIEW

## 2.1 Glutathione S-transferases

Glutathione S-transferases (GSTs; EC 2.5.1.18) that are distributed in nature are a diverse super family of detoxifying isoenzymes and being found in organisms as diverse as insects, fish, birds, microbes, plants, and mammals (Sheratt *et al.*, 2001). The transferases possess various activities and participate in different types of reaction. Plant GSTs include the five different classes which are phi, tau, theta, zeta and lambda classes; the theta and zeta have counterparts in animals whereas both of the sigma and theta classes are abundant in non-vertebrate animals (Nebert & Vasillou, 2004).

### 2.1.2 Classification and phylogenetic relationships of GSTs

According to the proteins sequence and structure form, there are at least four major superfamilies GSTs being classified into four different groups such as cytosolic GSTs, microsomal GSTs, mitochondrial GSTs, and fosfomycin resistance protein (Skopelitou *et al.*, 2012). GSTs also known as canonical GSTs (cGSTs) and exist in either homodimeric enzymes or heterodimeric enzymes. Those in the same classes have more than 40% amino acid sequence identity and between the classes, proteins have less than 25% sequence identity. Besides that, the primary structures at the N-terminus active site are conserved within the classes. A catalytically essential tyrosine, serine or cysteine residue that involve in conjugation with thiol group of Glutathione tripeptide (GSH) are presence in the conserve N terminus structure (Oakley, 2011).

Within each of the classes or subfamilies consists about 90% similarity between separate, highly homogenous, polypeptides. Therefore, each class of the respective families can be classified using different structures of the genes, chromosomal localizations as amino acid residues at position 60 and 80 are well conserved (Sheehan

*et al.*, 2001). Immunoblotting technique uses to study both the tissue-specific expression of GSTs and the determination of immunological relationships.

Cytosolic GSTs (soluble GSTs) have formed the largest super family. Cytosolic GSTs are the first GSTs enzymes being found and studied. For now, the documented classes of cytosolic GSTs are alpha, beta, delta, epsilson, theta, mu, nu, omega, pi, sigma, tau, phi, and zeta (Oakley, 2011). The alpha, mu, pi, and theta class GST genes have different in size and cistrons structure. However, there are few classes of this superfamily, called Beta (prokaryotes), Chi (bacteria and insects), Delta, Epilson, Lambda, Phi, and Tau (plants) are restricted to non-mammalians species (Pandey *et al.*, 2015).

Eukaryotic GST enzymes include a complex enzyme family that has been subclassified into different types of classes based on types and sequence of amino acid, nucleotide sequence, immunological identity, substrate and inhibitor specificity, kinetic and primary and tertiary structural characteristics (Sheehan *et al.*, 2001). However, kinetics properties (substrate specificities and inhibitor sensitivities) could not differentiate clearly between the GST isoenzymes as most of them often overlapping and broad. Kinetics properties are important when studying mammalian GSTs where the level of sequence identity is low. Based on the measures and studies mentioned, the mammalian cytosolic GSTs are divided into few classes which are Alpha, Mu, Omega, Pi and Theta, and Zeta classes (Pandey *et al.*, 2015). This classification was established as protein sequence data with sequence identities of 60 to 90% at the protein level within respective class and between classes.

The mitochondrial GSTs (kappa class GSTs) are studied and purified from mammalian mitochondria which are soluble dimeric proteins. They have shown an example of evolutionary relationship with cytosolic GSTs as both GSTs have the ability

to form dimer. Besides that, the heterodimers of cytosolic GSTs have been studied containing chains belonging to the same class (Oakley, 2011).

The microsomal GSTs have special features as they are membrane-bound and they are classified as membrane-associated proteins in eicosanoid and glutathione metabolism (MAPEG). Furthermore, they are further divided into four subgroups (I-IV) and each of them have less than 20% sequence identity which have make a clear difference among them (Oakley, 2011). In human, more than six different types of MAPEG isoenzymes identified. Most of them are characterized and grouped under to I, II and IV, for example: 5-lipoxigenase activating protein (FLAP), leukotriene $C_4$ synthase. Some of the MAPEGs (example: MGST1) shared common characteristics with cytosolic and mitochondrial GSTs which can catalyse conjugation of GSH to electrophilic compounds. In the microsomal GSTs of rats, the activation conjugation between CDNB and GSH can be occurred through either alkylation of Cys-49 or limited proteolysis at Lys-4 or Lys 41 (Sheratt *et al.*, 2001). Most of the MAPEG members contribute in the biosynthesis of few chemical compounds, for examples, leukotrienes and prostanoids, endogenous lipid signaling particles.

Certain bacteria are grouped as MAPEG members such as *E.coli*, *Synechocystic* sp. and *Vibro cholera* as exhibited distant evolutionary relationships with the eukaryotic mammalian and some of them have multiple MAPEG paralogues. Bacterial MAPEG proteins have separated into two main discrete subfamilies. The representative of each group is *E.coli* and *Synechocystic* sp. protein (Allocati *et al.*, 2009).

Three families that mentioned above are clearly seen in different and present in prokaryotes however the forth family only can be found in bacteria. Takashi Shishido is the first researcher found and proven for the presence of GSTs activities in bacteria which is in the strain of *Escherichia coli* (Ziglari *et al.*, 2013). This have shown GSTs

have been found in aerobic prokaryotes, human, plant pathogens and soil bacteria (Allocati *et al.*, 2009).

There are different classes of cGSTs which can be found in bacteria and have been recognized based on their structural and catalytic properties which are beta, chi, theta and zeta. Multiple GST genes of widely divergent sequences and function are used to characterised and studied about bacteria and eukaryotic organisms. For examples, *Pseudomonas mirabilis* and *Proteus vulgaris* have more than three different GSTs.

Beta class cGSTs shows activity with substrate 1-chloro-2,4-dinitrobenzene (CDNB) and bind to the GSH-affinity matrix. This class of GSTs can be purified and characterized from *E.* coli, *Ochrobactrum anthropi* (OaGST) and *Bukholderia xenovorans* (BxGST). The first cGST of this class was characterized from a *Proteus mirabilis* strain (PmGST) that serves as a prototype of the beta class. Besides that, they additionally can be described by the cysteine residue located at the GSH site (Chee *et al.*, 2014).

Theta class compounds in microbes demonstrated high amino grouping comparability with eukaryotic theta class GSTs. Dichloromethane (DCM) dehalogenase generated by facultative methylotrophic microbes fills in as the case for this classes of GSTs. They have unmeasurable conjugation activity with CDNB and unable to bind to GSH affinity matrices which differentiate them from beta class GSTs. The theta class of GSTs includes certain bacterial GSTs and some plants, mammals, fish, birds, insects, yeasts, and fungi. Theta classes GSTs were the ancestor of the other classes of GST enzymes. However, we have limited knowledge of bacterial GSTs compared to their eukaryotic homologs, this suggests that GST genes have their primordial origin in bacteria (Vuilleumier, 1997).

Zeta class described by two serine and a cysteine amino acid residue located in N terminal site. Tetrachlorohydroquinione (TCHQ) dehydrogenase belongs to this class that have a role in the biodegradation of pentachlorophenol and isomerase reaction. (Anandarajah *et al.*, 2000).

Chi class cGSTs lack of cysteine residues completely even though they show typical structures features of cGSTs. This has indicated that these enzymes may have different evolutionary pathways from the beta class cGSTs. Two cyanobacterial cGSTs haven been purified and studied from *Thermosynechoccus elongates* BP-1 (TeGST) and *Synechoccus elongates* PCC 6301 (SeGST) (Panley *et al.*, 2015).

Fosfomycin resistance protein have a distinct difference in terms of primary sequence and in structure, therefore there were not measured in the phylogenetic tree.

### 2.1.3 General structural studies on GST enzymes

The conservation of the structural features was observed across all the classes of GST enzymes. This is to study both functional versatility and difference in sequence in the GST enzymes. GSTs with known structures from all classes are homodimeric enzymes in which each monomer folds into a two-domain conformation. The N-terminal domain consists of *bababba* unit are mostly the glutathione-binding site and whereas a-helical C-terminal domain is involved mainly in the attraction of hydrophobic substrates. From the past research, most of the residues that are extremely conserved in enzymes of the alpha, mu, theta and pi classes are not preserved in bacterial (Vuilleumier, 1997).

The mammalians cytosolic GSTs, especially those isoenzymes from alpha, mu, and pi class were structurally characterized because of their relevance to toxicology, disease, malignant cells and drug metabolism. The first structure being studied was the porcine pi-class enzyme (pGSTP1-1) as this isoenzyme contains the indicative features of members of the cytosolic GST superfamily and acts as feature to compare with other

isoenzyme, such as both of the structure of rat, rGSTK1-1 and human, hGSTK1-1 mitochondrial GSTs (Oakley, 2011). Structure of porcine pi-class enzyme (pGSTP1-1) has an N-terminal thioredoxin-like domain (with βαβαββα topology) and a C-terminal domain composed of α helixes.

In addition, a cis-proline residue is found N-terminal end of strand beta that forms hydrogen bond interactions with the backbone amine group of the GSH-cysteinyl moiety at the preliminary interaction found in all classes of cytosolic GSTs and mitochondrial GSTs. The greatest variability among the classes is the region containing helix α2 and the secondary structure part show activities with the glycine-residue of GSH. Based on the similarities between sequence and structural, cytosolic GSTs subdivided into two main groups which are Y-GSTs and S/C-GSTs. Y-GSTs will use a tyrosine residue in their sequence to active glutathione while S/C-GSTs have a serine amino acid or the cysteine residue in both beta- and omega-class GSTs. The hydroxyl group of these residues will donate a hydrogen bond to the GSH sulfhydryl to promote the formation of thiolate anion. In both of the cytosolic and mitochondrial GSTs, the catalytic GSH-activating residue occurs in a "catalytic loop" following the first β-strand in the thioredoxin-like domain. Alpha, mu, pi, sigma-class isoenzymes in human are classified under Y-GSTs while the other classes of GST group under S/C-GST family (Allocati *et al.*, 2009).

The isoenzymes of the mitochondrial GSTs similar with the theta class GSTs as they have a GSH-activating serine residue whereas the omega-GSTs quite similar with beta class GSTs and glutaredoxins as they can utilize cysteine residues and form a mixed disulfide with GSH.

Furthermore, in year 1992, through the crystal structure of the human cytosolic pi class GST (hGSTP1-1) that was co-crystallized with S-hexyl glutathione, binding site for hydrophobic co-substrates has identified and it was located adjacent to the G-site

and form a gap in between the N and C terminal domains. The binding site for hydrophobic co-substrate differs greatly in shape and chemical character among the classes (Oakley, 2011).

MAPEG protein structure was studied through the determination of MGST1 from rat at 3.2/4.0 Å resolution by electron crystallography, the X ray crystal structures of human $LTC_4$ synthase ($LTC_4$-S) in its apo and GSH-complexed forms at 2.00 Å, 2.15 Å, and 3.3 Å resolution. Few crystallographic researches on different MAPEG members have showed that mostly are left handed four $\alpha$ helix bundles (TM1, TM2, TM3 and TM4) arranged into trimers, with the helical bundles oriented orthogonally in the plane of the membrane. The overall topology of both MGST1 and $LTC_4$-S are quite similar to subunit I of ba3-cytochrome c oxidase. There are three GSH binding sites per trimer which located proximal to the cytoplasmic side of the predicted membrane-spanning regions. The MGST1 structure proposed that GSH was attached in an extended conformation which is similar in c- and mitochondrial GSTs, whereas in $LTC_4$-S structures, it has higher resolution and it is in V-shaped conformation with its thiol group oriented toward the membrane where it can presumably interact with its membrane bound substrate.

Most of the bacterial GSTs identified to date belong to the bacteria-specific beta class. There are four representative crystal structures of beta class GSTs have been studied: *P.mirabilis* GST (PmGST) (Allocati *et al.*, 2012), *E.coli* (EcGST) (Nishida *et al.*, 1998), *B. xenovorans* (BxGST) (Hofer *et al.*, 1994) and *O. anthropi* (OaGST) (Favaloro *et al.*, 1998). Using both of the crystal structure and site-directed mutagenesis, the structural and catalytic properties of the beta class enzymes can be studied (Allocati *et al.*, 2009).

Beta class cGSTs are homodimers with a chain length of 201-203 residues and they have a thioredoxin-like N-terminal domain and an all-helical C-terminal domain separated by a short linker. Furthermore, they are well categorized by the existence of a conserved cysteine (amino acid) residue located close to the GSH sulfydryl group which have mentioned previously. Comparing the crystal structures, the overall structure in beta class GSTs is highly conserved. When the protein monomers are superimposed, the root mean square deviations among equivalent Cαs are about < 1.5Å even though their sequence identities are < 35-40%. Besides that, when beta class monomers are superimposed onto cGSTs belonging to other classes, the root mean square deviations increase, which is about 1.85 to 2.67 Å. From the studies, these values have indicated that the canonical fold has been preserved from bacteria to mammals.

### 2.1.4 Roles of GSTs

The primary basis for all GST catalytic activities is the ability of these enzymes to lower the pKa of the sulfhydryl group of reduced glutathione (GSH) from pH 9.0 in aqueous solution to about pH 6.5 when GSH is bound to their active site (Winayanuwattikun *et al.*, 2005). Glutathione S-transferases (GSTs) catalyses the conjugation of reduced tripeptide glutathione (GSH) with compounds that contain an electrophilic centre through formation of a thioether bond between the sulfur atom of the GSH and the substrate or the reactive oxygen species (ROS), majority of the substrates are xenobiotics or products of oxidative stress (Sheratt *et al.*, 2001). In other words, GSTs are multifunctional enzymes that serve as catalytic functions in many processes, including cellular protection from ROS, reductive maintenance of thiolated proteins prostaglandin synthesis, and glutathione conjugation of endogenous and exogenous ligands. These enzymes also have several non-catalytic functions that help in the sequestering of carcinogens, intracellular support of a broad spectrum of hydrophobic ligands, and modulation of signal transduction pathways (Shi *et al.*, 2014).

Glutathione *S*-transferases (GSTs) have been studied in eukaryotes since their discovery in 1961 because of their involvement in the metabolism of xenobiotics. At year 1961, the extracts from rat liver were successfully studied on catalyzing the conjugation of GSH with both 1, 2-dichloro-4-nitrobenzene, DCNB and bromosulphophthalein (BSP). After purified and characterized the protein, it was shown to be part of class Mu of the cytosolic GST superfamily (Booth *et al.*, 1961). Even though 1-chloro-2,4-dinitrobenzene (CDNB) is recognised as the greatest shared transferase substrate facilitated identification of Alpha, Pi, Sigma, Kappa and Mu class family, Theta class were first purified using 1-menaphthyl sulfate and 1,2-epoxy-3-(p-nitrophenoxy) propane as substrates. Besides that, both of the Zeta and Omega GST classes were characterized using a bioinformatics approach.

In higher eukaryotes, GST enzymes serve as major phase II detoxification enzymes that are mainly found in cytosol and take part in binding, transformation, and detoxification of a wide variety of both endogenous and exogenous electrophilic compounds. These enzymes are usually active as dimers (homodimeric or heterodimeric GSTs) and catalyse the binding between tripeptide glutathione and a wide variety of biologically active molecules carrying an electrophilic centre. Most of them are xenobiotics or the products of oxidative stress. Therefore, the xenobiotic-conjugate will be removed from the cell during the phase III of drug metabolism (Sheehan *et al.*, 2001).

Once the compounds have transported out of the cell, the peptide of the GSH-conjugates will attack by the γ-glutamyltransferase peptide and either aminopeptidase M or cysteinylglycine dipeptidase to form a cysteinyl conjugate which in turn N-acetylated to produce a mercapturic acid that is typically the final product to be excreted from the body in urine. GST enzymes can either be expressed constitutively or be induced by a wide range of compounds of both natural origin and xenobiotic origin and most of the known substrates of GSTs are xenobiotic synthetic chemicals as the xenobiotics may

interact deleteriously with an organism, causing toxic and may lead to carcinogenic effects. Some of these xenobiotic compounds that may arise during oxidative damage to cell components, such as endogenous lipids, DNA hydroperoxides, and hydroxyalkenals or steroids, leukotrienes, anthocyanines, and organic isothiocyanates. All these are the examples for other natural GST substrates. Besides that, various GST catalysts have the ability to attach lipophilic chemical that have a role ligand however not as substrates (Vuilleumier, 1997).

Most classes of cytosolic GSTs in human mainly involve in the metabolism of drugs and foreign chemicals, for instances, carcinogens, environmental pollutants, cancer chemotherapeutic drugs and detoxification of some harmful endogenously derived reactive compounds. Besides that, some of the cytosolic GSTs also helped in synthesis and inactivation of prostaglandins. Isoenzymes of class alpha and zeta possess GSH-dependant isomerization activities; the sigma class GSTs known as hematopoietic prostaglandin D synthase catalyses $PGH_2$ to form $PGD_2$ with the presence of GSH. A few of the theta class GST isoenzymes have sulfatase activity while omega class GSTs have some common features with glutaredoxins which form mixed-disulfides with GSH and catalyse reductase reactions (Oakley, 2011).

In bacteria, the beta class GSTs are involved in variety activities such as protection against chemical and oxidative stresses, antimicrobial drug resistance and in the catabolism of xenobiotics. Because of their unique and useful roles in detoxification of a wide variety of xenobiotics, bacterial GSTs could potentially be beneficial in designing genetically modified organisms for use in bioremediation and degrading organic pollutants found in the environment (Chee *et al.*, 2014).

Bacterial GSTs are involved in degradation of xenobiotics, protection against chemical and oxidative stresses, cellular protection from reactive oxygen species, and antimicrobial drug resistance. In addition to their role in detoxification, bacterial GSTs also implicated in some of the metabolic mechanisms, for example, biotransformation of dichloromethane, the degradation of lignin and atrazine, and the reductive dechlorination of pentachlorophenol. Furthermore, several bacterial GSTs take part in aerobic degradation of different aromatic compounds such as biphenyls and polyaromatic hydrocarbons (Allocati *et al.*, 2009).

The association of bacterial GSTs in degradation of toxic pollutants have indirectly suggests a role for bacterial GSTs in biodegradation, with potential in bioremediation. Using bacterial systems based on GSTs to screen and select may yield new catalysts for the detoxification of harmful chemicals and toxic pollutants.

### 2.1.5 Fosfomycin resistance

Fosfomycin resistance protein is one of the large superfamilies of GSTs and they are mainly chromosomal. However, their resistance genes have also been found on transmissible plasmids and can be achieved by different mechanisms. There are three different mechanisms of resistance towards the modification and inactivation of fosfomycin have been found: decreased uptake of the antibiotic, overexpression or mutation of MurA and enzyme modification of the antibiotic (Nikolaidis *et al.*, 2014).

Research have been made in the nutrient transport systems for fosfomycin uptake of *E.coli*. Both of the L-α-glycerol-3-phosphate transporter (GlpT) and the glucose-6-phosphate transporter (UhpT), hexose phosphate transporter are the major transporters in the system (Kurahayashi *et al.*, 2014). The expression of both the GlpT and UhpT transporters is stimulated by their substrates, glycerol-3-P and glucose-6-P, respectively, and requires the presence of cAMP-CR (Karageorgopoulos *et al.*, 2011). Therefore,

when there is mutation occurred in any of the structural genes of those pathways, it will reduce permeability to fosfomycin, decrease in antibiotic uptake, and confer different levels of fosfomycin resistance (Castaneda *et al.*, 2013). As a result, strains defective in fosfomycin uptake are not able to grow using glycerol-3-P as substrate in GlpT-deficient strains or glucose-6-P (and other hexose phosphates) substrate in Uhp-deficient strains. Therefore, the measurement of MIC to fosfomycin in *E. coli* is performed using media with and without glucose-6-P. This is because the addition of glucose-6-P provides a more reliable MIC result, due to its activity as inducer of fosfomycin transport.

The second type is the overexpression or mutation of MurA which were remained catalytically active yet resistant to attack of the fosfomycin. The chemical structure of fosfomycin mimics both glycerol-3-P (G3P) and glucose-6-P (G6P) and transports under normal conditions without being detected by those transported. In the first step of the peptidoglycan biosynthesis, MurA catalyse the formation of a peptidoglycan precursor (UDP-GlcNac-3-O-enolpyruvate) from UDP-GlcNAc and PEP under normal condition. However, when fosfomycin is present and transport inside the cell by GlpT and UhpT, it will block the UDP-GlcNac-3-O-enolpyruvate synthesis by mimicking the PEP which serves as original substrate of MurA. This has inhibited cell wall synthesis and leading to cell death. There are two different studies on the second type mechanisms using *E. coli* and *P. aeruginosa.* In *E.coli*, fosfomycin uptake depends on GlpT and UhpT while in *P. aeruginosa*, fosfomycin can only enter into the cells via GlpT due to the absence of UhpT permease. This has indicated that *glpT* is the only target gene whose inactivation confers antibiotic resistance in *P. aeruginosa* (Castaneda *et al.*, 2013).

The third type of fosfomycin resistance protein which is a metalloenzyme superfamily. There are 3 members found in this family which are Fos A, Fos B and Fos X based on sequence homology, metal preferred for catalysis, and choice of nucleophile conjugated to fosfomycin. They also known as vicinal oxygen chelate superfamily (VOC) as they share a common structural fold that provides a flexible metal coordination environment, facilitating the catalysis. The enzymes of this family use both histidine and glutamate residues to bind metal ions and they contain conserved βαββββ structural motifs which pair to form a cupped-shaped metal binding site.

Fosfomycin A was originally recognized in conjugative multi-resistance plasmids from *Enterobacteriaceae* clinical isolates. Due to the unique enzymatic modification of fosfomycin, Suaraz and her co-workers established a new mechanism of antibiotic resistnace. Inactivation of fosfomycin happened because it can conjugate with tripeptide glutathione (γ-Glu-Cys-Gly, GSH), catalyzes the covalent bond between the sulfhydryl deposit of the cysteine in glutathione and the C-1 of epoxide component of fosfomycin.. The resulted opening of the epoxide ring of the antibiotic form an inactive adduct and it was eventually proven by the nuclear magnetic resonance (Ziglari *et al.*, 2013). GST enzyme catalyzed the reaction. This enzyme was purified and characterized. The purified GST enzyme did not bind to the GSH-agarose matrix and did not catalyze the reaction between GSH and CDNB. Thus, these have indicated that this protein had different properties from the cGSTs. It is a 32kDa soluble homodimer protein (Allocati *et al.*, 2009).

FosA serves as homodimeric metalloenzyme that can interact stronygly with with the substrate fosfomycin and the enzyme as a $Mn^{2+}$ or $Co^{2+}$ molecule bound to each subunit in a metal binding site. According to Bernat (2001), a monovalent potassium cation, $K^{+}$ is vital for optimal activity (Bernat *et al.*, 2001). In other words, it is a $Mn^{2+}$ or $Co^{2+}$ dependent glutathione S-transferase that inactivates fosfomycin by the addition of

glutathione to the oxirane ring of fosfomycin. In subsequent studies, Armstrong and co-workers identified that Fosfomycin A (FosA) is a metalloglutathione transferase identified with both glyoxalase I and extradiol dioxygenases which are the individuals from the vicinal oxygen chelate superfamily.

Besides that, FosA is found in the bacterial genomes and the 3D structure of a genomically encoded FosA from the pathogen *Pseudomonas aeruginosa* was studied. The protein fold showed the conserved βαββββ structural motifs that form a cupped-shaped metal binding site. The $K^+$ ion is accommodated in a loop located 6.5Å from the $Mn^{2+}$ cation. In addition, the structure of FosA in complex with antibiotic was also identified. Both of the plasmid-encoded and genomically encoded enzymes are very similar in structure. This has been showed in the crystal structure of FosA from transposon Tn2921 as it maintains the same basic molecular arrangement observed in genomically encoded FosA. Based on the structural data, the residues involved in the binding of both fosfomycin and GSH substrates have been discovered and characterized by mutagenesis.

FosB was firstly found in a plasmid conferring resistance to fosfomycin in *Staphylococcus epidermidis* and the gene was encoded by plasmids. Besides that, it has been found in chromosomes and plasmids of most of the Gram-positive bacteria such as *Bacillus anthracis*, *Bacillus cereus*, *Bacillus subtilis*, *E.* faecium, and *S. aureus*. In *B. subtilis*, expression of FosB gene in bacterial chromosome involves the extra cytoplasmic transcription sigma factor, σW, a regulator that provide inducible bacterial defense mechanisms against antimicrobial compounds (Rigsby, 2009). FosB was initially characterized as an $Mg^{2+}$ dependent L-cysteine thiol transferase that catalyzes the addition of a thiol group to fosfomycin using L-cysteine as a thiol donor substrate. This is because most of the Gram-positive bacteria lack the genes necessary for GSH synthesis. They do not have GSH molecules. The activity of FosB in *B. subtilis* has

been reported that 10-fold greater with the presence of $Mg^{2+}$ or $Ni^{2+}$ than with $Mn^{2+}$ as a cofactor. The protein has little activity with Mn(II) compared to $Mg^{2+}$ as its cofactor. However, FosB shows no activation by monocovalent metal cations.

Bacillithiol, the α-anomeric glycoside of L-cysteinyl-D-glucosamine with L-malic acid could be the thiol donor *in vivo* for FosB. This has been shown when the cells lacked bacillithiol, the sensitivity towards fosfomycin increase in *B. subtilis*, *B. anthracis* and *S. aureus*. In addition, kinetic analysis of FosB from *S. aureus* has proven that the enzyme is a dimeric metallothiol transferase ($Mg^{2+}$ and $Mn^{2+}$) thiol S-transferase, and bacillithiol is its preferred thiol substrate under physiological conditions.

FosX hydrolases are a subfamily of enzymes associated to FosA and FosB. FosX hydrolases sharing 30%–35% sequence identity with both groups of enzymes. FosX is a Mn (II) dependent fosfomysin specific epoxide hydrolase that catalyses the hydration of fosfomycin by mediating the addition of water to the $C_1$ position of the antibiotic, breaking the oxirane ring, and producing a diol product (Casteneda *et al.*, 2013). In the reaction, an essential glutamic acid residue in the FosX active site acts as a general base catalyst. The enzyme is genomically encoded and those *FosX* homologues are well characterized, such as *Mesorhizobium loti*, and the pathogens, *Brucella melitensis*, *Clostrium botulinum*, and *Listeria monocytogene* (Fillgrove *et al.*, 2007). *L. monocytogene* FosX is a good catalyst and it has high resistancy towards fosfomycin while *M. loti* FosX produces modest resistance to the antibiotic and its kinetic constant is lower than *L. monocytogene* FosX. Furthermore, the structure of FosX was also identified and it was very similar with FosA from *P.aeruginosa*. However, FosX enzymes do not contain a $K^+$ ion binding site near to the active site. Other than this, FosX enzymes bind to the fosfomycin in a different orientation from that observed in the FosA enzymes.

There is a new mechanism of fosfomycin inactivation was characterized which can be found in a fosfomycin-resistant strain of *Pseudomonas syringae*. FosC can be found in this bacterial which inactivated the antibiotic using ATP to phosphorylate fosfomycin in the presence of $Mg^{2+}$. This was found out using the sequence alignments highlighting a region of partial homology between FosC and the Mg-ATP binding domains of AMP-ATP phosphotransferases. However, a recent article established that FosC from *P. syringae* is an ortholog of FosA (Nikolaidis *et al.*, 2014).

In short, FosA converts fosfomycin to fosfomycin monophosphate, whereas FosB produces fosfomycin diphosphate using the monophosphate form as a substrate. FosA shares homology with the FosC but differs from FosB. Intrinsic resistance to fosfomycin in *P. syringae* relies on a fosfomycin kinase named FosC, by phosphorylating the antibiotic to produce fosfomycin monophosphate with presence of ATP in the reaction.

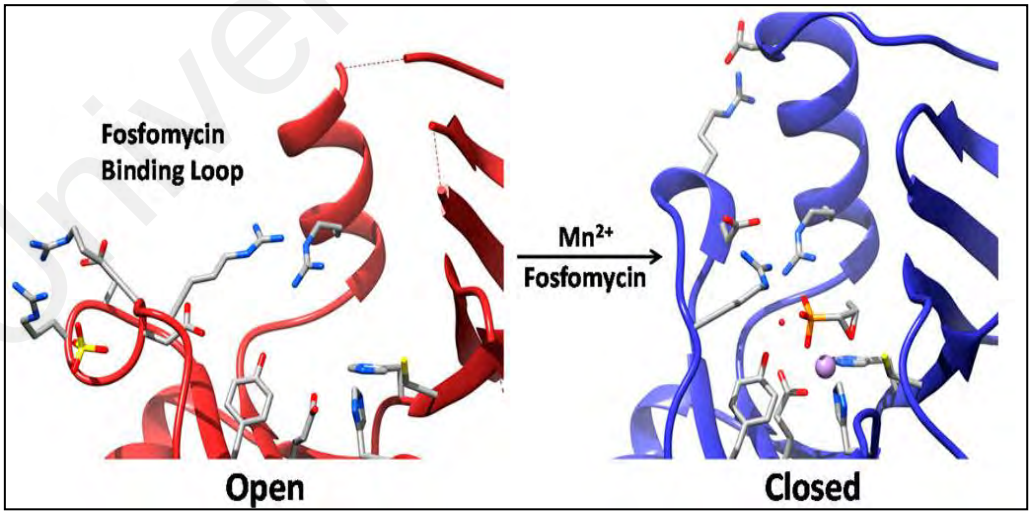


**Figure 1.1**: Two different conformation of the FosB. $Mn^{2+}$ and fosfomycin are bound in the active site and the conserved phosphonate binding loop is observed in the closed conformation (Right). No metal or antibiotic bound in the active site and the phosphonate binding loop is observed in the open conformation (Right) (Thompson *et al.*, 2014).

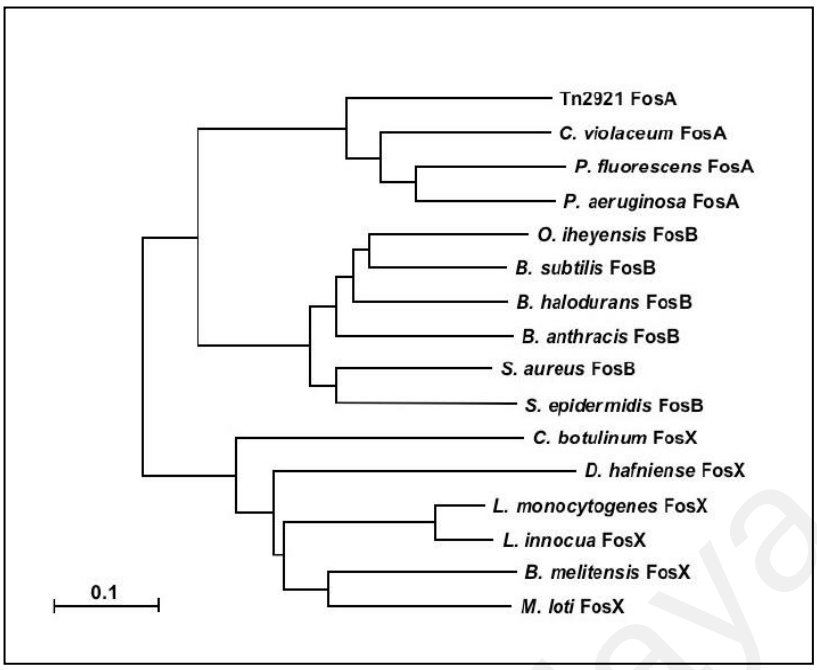


**Figure 1.2**: Relationship between the fosfomycin resistance proteins which can divided into three classes based on sequence homology, metal preferred for catalysis, and choice of nucleophile conjugated to Fosfomycin (Rigsby, 2009).

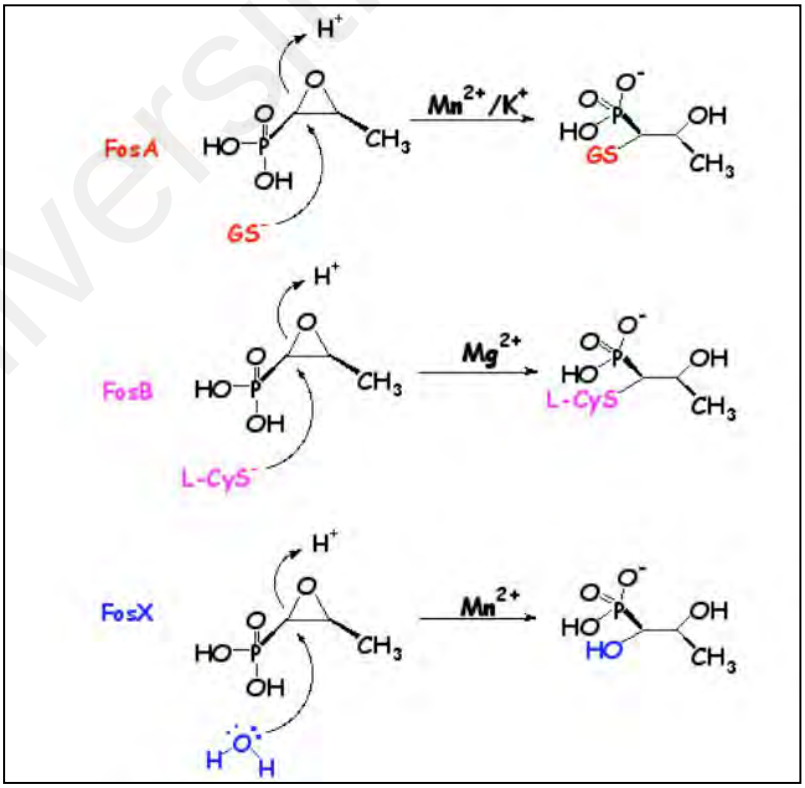


**Figure 1.3**: A summary of the reactions catalyzed by each classes (FosA, FosB and FosX) (Rigsby, 2009).

### 2.1.6 Potential applications of bacterial GSTs

As a summarized of what have described previously, bacterial GSTs are mainly involved in several types of chemical transformations and detoxification. These have shown that bacterial GSTs may represent a versatile tool with a variety of biotechnological applications, for example, in the field of bioremediation, an economical alternative to conventional physicochemical methods to clean up environmentally contaminated sites (Chee *et al.*, 2014).

As their genetic can be easily manipulated and grew rapidly, these have become the advantages to study and exploiting the potential biotechnological applications of using engineered proteins and bacterial strains. The combination of both molecular biological and protein chemical techniques have identified and characterized bacterial GST enzymes at an increasing rate. Several studies have been carried out using both purified proteins and microorganism engineering in order to explore and enhance the application of bacterial GSTs. For example, using DNA shuffling technique to obtain chimeric enzymes with improved catalytic properties and altered substrate selectivity towards several noxious iodoalkanes (Mannervik *et al.*, 1985) and creating fusion proteins with several distinct enzymatic activities (trifunctional enzyme with superoxide dismutase, glutathione peroxidase and glutathione transferase). All these studies have shown indirectly that bacterial GSTs may have several applications in medicine as well as in environmental field.

Besides that, there is another application of bacterial GSTs lies in the preparation of biosensors. Biosensors are an inexpensive method to check and detect targeted contaminants in environment. Biosensors are easy to use, environmentally friendly and characterized by high sensitivity and selectivity as compared to conventional methods. One of the examples is a mammalian GST was used to develop an optical biosensor for

detection of captan in contaminated waters. Captan is a strong inhibitor of GSTs and it used to control some of the plant pathogenic microorganisms.

The development of screening and selection programs using bacterial systems based on GSTs may yield new catalysts for the detoxification of environmental toxic compounds. For example, a single bacterial strain can be engineered to carry a complete metabolic pathway that efficiently eliminates environmental toxic compounds. *E. coli* is engineered for improving the degradation of chlorinated ethenes, which constitute a large group of toxic environmental pollutants (Wood, 2008). They have constructed a recombinant *E. coli* strain in which a toluene ortho-monooxygenase from *Burkholderia cepacia* G4 (Rui *et al.*, 2004) and a GST from *Rhodococcus* AD45 with activity towards cis-1,2-dichloroethylene epoxide and epoxypropane, were co-expressed (Wood, 2008). As a result, the recombinant GST strain able to transform and eliminate the reactive intermediate epoxide in *E.coli*. The examples provided above highlight bacterial GSTs constitute an effective resource in detoxification for the future.

The conjugation and detoxification of herbicides and pesticides by bacterial GSTs is an area where most of the researchers and interest to. Some of the rhizospheric Gram negative bacteria GSTs are involved in the detoxification and transport of pesticides and herbicides, in the metabolism of endogenous compounds, or in protection from pathogenic infection, often while stress-related responses.

Studies of bacterial GSTs may contribute new insights into the basic genetics and biochemistry of glutathione conjugate metabolism and the importance. Bacterial GSTs in our technological world also appears to be assured as suitable GST genes may be either recruited by screening or engineered by site-directed or random mutagenesis for applications in biodegradation or toxicology.

## 2.2 Plant growth-promoting bacteria (PGPB) *Pseudomonas* sp. UW4

The plant growth-promoting bacteria (PGPB) *Pseudomonas* sp. UW4 was obtained from University of Waterloo, Ontario, Canada. It was isolated from the rhizosphere of common reeds growing on the campus of the University of Waterloo which contribute to the development of plant growth-promoting mediated phytoremediation process (Duan *et al.*, 2013).

*Pseudomonas* sp. UW4 involved in bacterial heavy metal detoxification especially nickel, common stress adaptation, oxidative stress, and heavy metal efflux proteins. Presence of 1-aminocyclopropane-1-carboxylate (ACC) deaminase enzyme in *Pseudomonas* sp. UW4 catalyzes the deamination of ACC to produce α-ketobutyrate and ammonia. ACC is the immediate precursor of the phytohormone ethylene which produced and increased in amount result of various environmental stresses. *Pseudomonas* sp. UW4 attached to plant host surfaces can act as a sink for ACC to allow plants to maintain a beneficial level of ethylene without the risk of reaching inhibitory levels (Cheng *et al*., 2009). Due to the mechanisms of ACC deaminase enzyme, *Pseudomonas* sp. UW4 survive and resist towards nickel toxicity which is useful in phytoremediation.

Furthermore, *Pseudomonas* sp. UW4 considered as a novel bacterium as its complete sequence only revealed at year 2013 (Duan *et al.*, 2013). Genes in *Pseudomonas* sp. UW4 potentially involved in plant growth promotion are determined such as indole-3-acetic acid (IAA) biosynthesis, trehalose production, siderophore production, acetoin synthesis, and phosphate solubilization.

In *Pseudomonas* sp. UW4, production of IAA serves as a signal within the plant, directing both physiological and tropic responses to a range of environmental stimuli which influence most of the plant development such as cell division, elongation, fruit development, initiation of roots, leaves and flowers, cambial growth, vascular

development, and senescence (Duca *et al.*, 2014). Both indole-3-acetamide (IAM) and indole-3-acetaldoxime/indole-3-acetonitrile (IAOx/IAN) pathways of IAA biosynthesis are determined with the help of nitrilase and nitrile hydratase. Nitrile hydratase acts as an iron type metalloenzyme

Other than nickel metal, *Pseudomonas* sp. UW4 genes were also responsible for other heavy metal resistance such as copper, cadmium, zinc, molybdate, cobalt, arsenate, and chromate. By comparing the whole genome with other known *Pseudomonas* strains and phylogeny of four concatenated housekeeping genes which are 16S rRNA, gyrB, rpoB and rpoD of 128 Pseudomonas strains revealed that UW4 belongs to the *fluorescens* group, *jessenii* subgroup (Duan *et al.*, 2013).

In recent research shows that bioactive compounds produced by *Pseudomonas* sp. UW4 could be used for elimination of infections and treatment of breast cancer SK-BR3 (Parsiar *et al.*, 2016; Shahniani *et al.*, 2017). Metabolites of *Pseudomonas* sp. UW4 were isolated and tested on anti-cancer and anti-microbial activity which revealed the effect of metabolites of *Pseudomonas* sp. UW4 on breast cancer cells.

This project serves as a preliminary study of identifying putative GSTs of *Pseudomonas* sp. UW4 through bioinformatic analysis, purifying expressed GSTs from *Pseudomonas* sp. UW4 and characterizing the purified GSTs.

# CHAPTER 3: METHODOLOGY

## 3.1 Apparatus

BioRad Electrophoresis apparatuses (Biorad Laboratories Inc. California, USA.)

DEAE-Sepharose fast flow column (GE Healthcare, United Kingdom)

Filter paper (R & M Chemicals Ltd. Edmonton, Alberta)

Image Scanner III (GE Healthcare, United Kingdom)

Incubator (RS Biotech, United Kingdom)

Isoelectric focusing (IEF) apparatuses (Invitrogen, USA)

Laminar hood (Sastec, Malaysia)

Magnetic stirrer (Heidolph, Schwabach, Germany)

pI 3-10 IPG strips (GE Healthcare, United Kingdom)

Sodium dodecyl sulphate-polyacrylamide gel electrophoresis (SDS-PAGE) kits (Biorad Laboratories Inc. California, USA)

Tricorn$^{TM}$ 5/20 affinity column (GE Healthcare, United Kingdom)

UV Spectrophotometer (PerkinElmer, Inc., USA)

Vivaspin 6 protein concentrator (Sartorius, Gottingen, Germany)

## 3.2 Equipment

-20 ºC freezer (Denka, Japan)

4 ºC refrigerator (Protech, California, USA)

-80 ºC freezer (Denka, Japan)

Agar plates (Thermo Fisher Scientific, United Kingdom)

AKTA Purifier (GE Healthcare, United Kingdom)

Centrifuge machine (Thermo Fisher Scientific, United Kingdom)

Centrifuge machine (Eppendorf, Hamburg, Germany)

High-pressure steam sterilizer (Tomy, Japan)

Image Scanner III (GE Healthcare, United Kingdom)

Microwave oven (Pensonic, Malaysia)

Mili Q ultrapure water purification system (Milipore, Merck and Co., Inc, USA)

Multiphor II electrophoresis system (GE Healthcare, United Kingdom)

pH meter (Mettler Toledo, Ohio, USA)

Wise Bath Water bath incubator (Daigger Scientific Inc, US)

Water distiller (Favorit, Malaysia)

WISE-TIS Homogenizer HD-15G (Mega Lab, Greece)

## 3.3 Materials

0.5 M Tris HCl, pH 6.8 (Biorad Laboratories Inc. California, USA.)

1-Chloro-2,4-dinitrobenzene (Sigma Aldrich Co. USA.)

1.5 M Tris – HCl pH 8.8 (Biorad Laboratories Inc. California, USA.)

2,4-heptadienal (Sigma Aldrich Co. USA.)

30% Acrylamide (Biorad Laboratories Inc. California, USA.)

85% Hydrochloric acid (Merck and Co., Inc, USA.)

95% Ethanol (Systerm, Classic Chemicals Sdn. Bhd., Malaysia)

Acetone (Systerm, Classic Chemicals Sdn. Bhd., Malaysia)

Ammonium persulfate (APS) (Biorad Laboratories Inc. California, USA.)

Ampicillin, lysozyme (Invitrogen, Carlsbad, California, USA)

BenchMark$^{TM}$ Protein Ladder (Invitrogen, Carlsbad, California, USA)

Bovine Serum Albumin (Sigma Aldrich Co. USA.)

Bromophenol blue (Biorad Laboratories Inc. California, USA.)

Coomassie Brilliant Blue G-250 (Biorad Laboratories Inc. California, USA.)

Carrier ampholytes (Invitrogen, Carlsbad, California, USA)

CHAPS (Invitrogen, Carlsbad, California, USA)

Cumene hydroperoxide (Sigma Aldrich Co. USA.)

Dichlorodiphenyltrichloroethane (DDT) (Sigma Aldrich Co. USA.)

Ethacrynic acid (EA) (Sigma Aldrich Co. USA.)

Ethanol (Systerm, Classic Chemicals Sdn. Bhd., Malaysia)

Ethylenediaminetetraacetic acid (EDTA) (Sigma Aldrich Co. USA.)

Formaldehyde (Systerm, Classic Chemicals Sdn. Bhd., Malaysia)

Glacial Acetic Acid (R & M Chemicals Ltd. Edmonton, Alberta)

Glutathione reductase (Sigma Aldrich Co. USA.)

Glycerol (Systerm, Classic Chemicals Sdn. Bhd., Malaysia)

Glycine (Biorad Laboratories Inc. California, USA.)

GSH (Sigma Aldrich Co. USA.)

Hexadienal (Sigma Aldrich Co. USA.)

Hydrogen peroxide (Sigma Aldrich Co. USA.)

IEF Anode and Cathode Buffer (Invitrogen, Carlsbad, California, USA)

Iodoacetamide (Merck and Co., Inc, USA.)

Lysozyme (Sigma Aldrich Co. USA.)

Methanol (Systerm, Classic Chemicals Sdn. Bhd., Malaysia)

Nicotinamide adenine dinucleotide phosphate (NADPH) (Sigma Aldrich Co. USA.)

Ninhydrin (Sigma Aldrich Co. USA.)

N, N, N' N- tetramethylenediame (TEMED) (Biorad Laboratories Inc. California, USA.)

Novex IEF Pre-Cast Gel (Invitrogen, Carlsbad, California, USA)

Nutrient Broth (Merck and Co., Inc, USA.)

Nutrient Agar (Merck and Co., Inc, USA.)

Phenylthiourea (Sigma Aldrich Co. USA.)

p-nitrobenzyl chloride (NBC) (Sigma Aldrich Co. USA.)

Phosphoric Acid, 85% (Systerm, Classic Chemicals Sdn. Bhd., Malaysia)

Potassium Chloride (Merck and Co., Inc, USA.)

Protease inhibitor cocktail for general (Sigma Aldrich Co. USA.)

SERVA$^{TM}$ IEF marker (Invitrogen, Carlsbad, California, USA)

Silver nitrate (Systerm, Classic Chemicals Sdn. Bhd., Malaysia)

Sodium carbonate (Merck and Co., Inc, USA.)

Sodium dedocyl sulfate (SDS) (Biorad Laboratories Inc. California, USA.)

Sodium hydroxide (Merck and Co., Inc, USA.)

Sodium phosphate dibasic (Systerm, Classic Chemicals Sdn. Bhd., Malaysia)

Sodium thiosulphate (Systerm, Classic Chemicals Sdn. Bhd., Malaysia)

Sulfobromothaphlein disodium salt (BSP) (Sigma Aldrich Co. USA.)

Tetramethylethylenediamine (TEMED) (Biorad Laboratories Inc. California, USA.)

Trans-4-phenyl-3-butene-2-one (PBO) (Sigma Aldrich Co. USA.)

Trans-2-octenal (Sigma Aldrich Co. USA.)

Trichloroacetic Acid (R & M Chemicals Ltd. Edmonton, Alberta)

Tryptic Soy Agar (TSA) (Merck and Co., Inc, USA.)

Tryptic Soy Broth (TSB) (Merck and Co., Inc, USA.)

Ultrapure Urea (R & M Chemicals Ltd. Edmonton, Alberta)

β-Mercaptoethanol (Merck and Co., Inc, USA.)

### 3.4 Software

Mega7

Microsoft Excel

Phyre2

## 3.5 Methods

### 3.5.1 Bacterial sample collection

*Pseudomonas* sp. UW4 pure culture was obtained from University of Waterloo. A single colony was streaked out from the sample given and cultured on the sterilised tryptic soy agar (TSA) containing 100 μg/ml Ampicillin for 24 hours at 30 °C, followed by sub-cultured again on the tryptic soy agar at the same condition. The subculture procedures were repeated twice. *Pseudomonas* sp. UW4 stock samples were then prepared by mixing the broth culture with 50 % (v/v) sterilised glycerol and stored in the -80 °C freezer. *Pseudomonas* sp. UW4 samples were also cultured on the sterilised tryptic soy agar (TSA) containing 100 μg/ml Ampicillin for 24 hours at 30 °C and stored at 4 °C cold room for protein extraction and characterization.

#### 3.5.2.1 Protein extraction

A colony was chosen from the plate and cultured aerobically in the 150 mL sterilized tryptic soy broth containing ampicillin sodium (100 μg/ml) for 24 hours at 30 °C, followed by sub-cultured 50 mL into 1 L of sterilized tryptic soy broth containing ampicillin sodium (100 μg/ml) respectively and incubated for another 48 hours at 30 °C. Total 2 L of sample was cultured. The culture was then centrifuged under 6000 rpm, 15 minutes at 4 °C. The collected cell pellet was washed and well suspended in 5 mL of cold 25 mM of sodium phosphate buffer (pH 7.4). All samples were combined and centrifuged under 6000 rpm, for 45 minutes at 4 °C. 9.4 mL of cold homogenizing buffer (25 mM sodium phosphate buffer (pH 7.4) containing 1 mM EDTA, 0.1 mM DTT, 0.1 mM PTU and protease inhibitor, was added into the cell pellet and well mixed. 100 μL of 1 mg/ml muramidase (Fluka Analytical – 96381 U/mg) was then mixed into the sample and left for 45 minutes at room temperature. The suspended cells were disrupted by homogenization using WISE-TIS Homogenizer HD-15G and 500 μL of

CelLytic™ B Cell Lysis Reagent was then added into the sample and left for 15 minutes, under room temperature. The particulate material was removed by centrifugation at 6000 rpm for 1 hour at 4 °C (Simatani *et al.*, 2016). The supernatant was collected and applied to affinity column which was pre-equilibrated with eluting buffer.

#### 3.5.2.2 Purification of GSTs by using sulfobromothaphlein disodium salt (BSP) affinity chromatography

Fast protein liquid chromatography (FPLC) was washed with 20 % (v/v) ethanol, distilled water, followed by eluting buffer (cold 25 mM of sodium phosphate buffer, pH 7.4). Sulfobromothaphlein disodium salt (BSP) matrix column was used to trap and purify GSTs from the sample (supernatant collected from previous step). The packed BSP column was then coupled to AKTA Purifier™. The washing and equilibrating steps are using eluting buffer at flow rate 0.3 ml/min. The sample was injected into the affinity chromatography with flow rate 0.3 ml/min (Figure 3.1, Step I and II). Next, the sample was eluted with eluting buffer containing 0.5 M potassium chloride to remove all the unwanted protein that bound to the BSP matrix and the flow rate was set at 0.30 ml/min (Figure 3.1, Step III). The flow through was not collected. BSP column with bound GSTs was eventually eluted with eluting buffer containing 2 mM BSP as shown in Figure 3.2 and stored in 4 °C. While collecting the purified sample, the DEAE-sepharose fast flow column was attached below the BSP matrix column and both connected columns were pre-equilibrated with eluting buffer. All the purified protein was stored in 4 °C for substrate specificity determination or stored at −20 ◦C until further analysis.

The BSP dye that remained bound to BSP matrix column was washed using distilled water. While the remained BSP dye in the Hi-Trap DEAE Sepharose fast flow column was washed using eluting buffer containing 5 M KCl first then washed and filled the column with 20 % (v/v) ethanol. All the washing steps are using flow rate 0.3 ml/min.

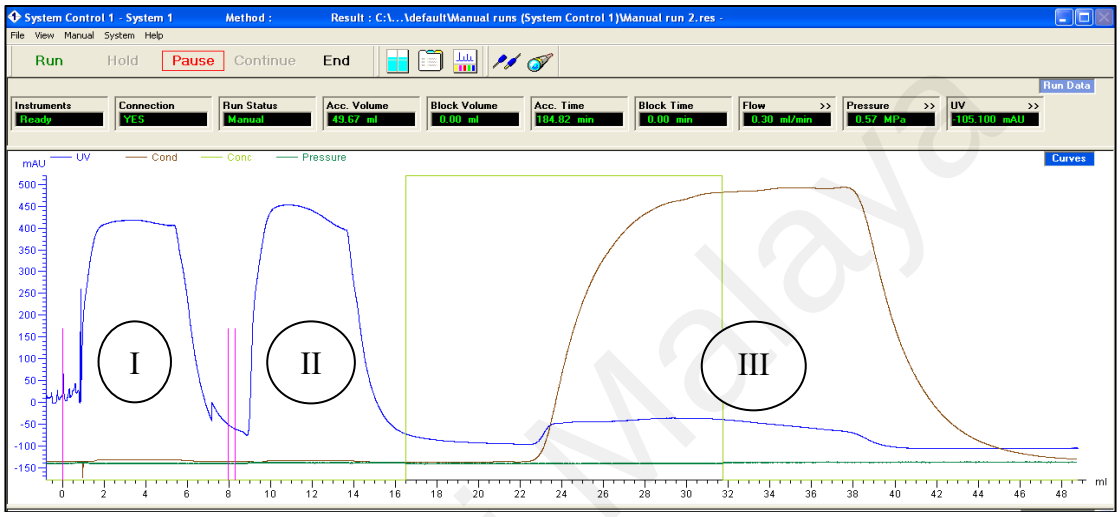


**Figure 3.1**: Injection of sample (crude) and washing of unwanted protein using 0.5 M KCl. Stage I and II show the injection of samples with flow rate 0.3 ml/min. Stage III shows the washing steps process using 0.5 M KCl with flow rate 0.3 ml/min.

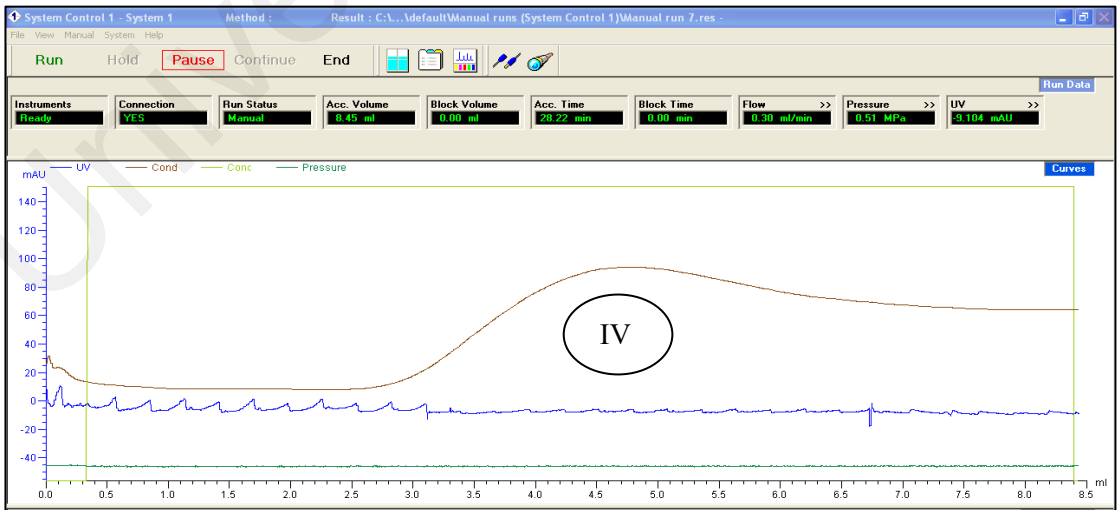


**Figure 3.2**: Elution of bounded GST protein from specific affinity column. Stage IV shows the elution of bounded purified protein with flow rate 0.3 ml/min.

### 3.5.2.3 Purification of GSTs by using GSTrap™ affinity chromatography

Fast protein liquid chromatography (FPLC) was washed with 20 % (v/v) ethanol, distilled water, cold 25 mM of sodium phosphate eluting buffer, pH 7.4. GSTrap™ affinity column was used to trap and purify GSTs from the sample. It was connected to AKTA Purifier™ and equilibrated using eluting buffer at flow rate 0.3 ml/min. The sample was then injected into the affinity chromatography with flow rate 0.3 ml/min. In order to remove untargeted protein that bound to the GSTrap™ matrix, the sample was eluted with eluting buffer containing 0.5 M potassium chloride and the flow rate was set at 0.30 ml/min. The eluent was not kept. GSTrap™ affinity column with bound GSTs was then eluted with eluting buffer solution containing 2mM GSH and kept in cool room with constant temperature 4 °C. All the purified protein was stored in 4 °C for substrate specificity determination or stored at −20 ◦C until further analysis (Harper & Speicher, 2011).

GSTrap™ was washed using distilled water at flow rate 0.3 ml/min and eventually filled with 20 % ethanol (v/v) before store inside the cold room.

### 3.5.2.4 Purification of GSTs by using Dinitrophenol (DNP) affinity chromatography

Fast protein liquid chromatography (FPLC) was washed with three solution which are 20 % (v/v) ethanol, distilled water, and eluting buffer. Dinitrophenol (DNP) matrix column was packed then coupled to AKTA Purifier™. The washing and equilibrating steps of column were done by using eluting buffer at flow rate 0.3 ml/min. The sample was injected into the affinity chromatography with flow rate 0.3 ml/min then eluted with eluting buffer containing 0.5 M potassium chloride with the flow rate 0.3 ml/min. The flow through was not collected because it contains all the unwanted protein. DNP

column with bound GSTs was then eluted with eluting buffer containing 2 mM GSH. All the purified protein was stored in 4 °C for substrate specificity determination or stored at −20 ◦C until further analysis.

#### 3.5.2.5 Protein Determination

Protein concentration was assayed by the Biuret method, using Coomassie Brilliant Blue R-250 and bovine serum albumin was used as the standard protein. Aliquots of bovine serum albumin (BSA) stock (1 mg/mL) and sample were pipette into test tubes and the total volume was made 100 $\mu$L by addition of distilled water. To every sample and standard, 5mL of Coomassie blue reagent was added, followed by vortexing. After 5 minutes, the absorbance was read at 595 nm. The amounts of BSA in the standards were plotted against their average absorbance. The protein content of the samples was estimated from the standard curve (Chee *et al.*, 2014).

### 3.5.3 Protein Characterization

#### 3.5.3.1 Molecular weight determination by using SDS-PAGE

##### 3.5.3.1.1 Preparation of the gel

Both resolving gel (12% w/v) and stacking gel (4% w/v) were prepared as shown in the Table 3.1. Both APS and TEMED were added lastly and stirred gently. Resolving gel (12%) solution was pipetted slowly into the space in the middle of the glass plates to keep any formation of air pockets and polymerize before including the stacking gel (4%) arrangement onto the gel (Pandey *et al.*, 2015).

**Table 3.1**: Volume and composition of solution used in preparing 4% stacking gel and 12% resolving gel.

| Solution | Resolving gel (12%) | Stacking gel (4%) |
|---|---|---|
| Distilled water | 3.40 mL | 6.10 mL |
| 30 % acrylamide | 4.00 mL | 1.30 mL |
| 1.5 M Tris pH 8.8 | 2.50 mL | - |
| 0.5 M Tris pH 6.8 | - | 2.50 mL |
| 10 % SDS | 0.10 mL | 0.10 mL |
| APS | 50.00 µL | 50.00 L |
| TEMED | 5.00 µL | 10.00 L |

**Table 3.2**: Volume of solution to prepare 1 x SDS sample buffer.

| Reagent | Volume |
|---|---|
| Distilled water | 3.55 mL |
| 0.5 M Tris-HCl, pH 6.5 | 1.25 mL |
| Glycerol | 2.50 mL |
| 10 % (w/v) SDS | 2.00 mL |
| 0.5 % (w/v) Bromophenol blue | 0.20 L |
| β-mercapethanol | 5.00 L |
| **Total volume** | 14.50 mL |

The purified protein was concentrated using Vivaspin 6 protein concentrator, followed by dilution (1:1 ratio) with the sample buffer and heated at 95°C for 4 minutes. 1 x SDS sample buffer was made as shown in Table 3.2. The prepared gel was placed inside SDS tank. The electrophoresis running buffer was prepared (Appendix B). It was poured and covered the inner tank. After the comb has been removed carefully, 0.8 µL marker and 20 µL purified protein sample from FPLC were loaded into the well respectively. The purified sample was went through electrophoresis process at 120V under room temperature. BenchMark™ serves as a molecular size marker in this studies. After 1.5 hours, Vorum silver stain method (Table 3.3) was used to stain the gel for viewing purposes.

**Table 3.3**: Vorum Silver stain method.

| Stage | Reagents | Volume | Time |
|---|---|---|---|
| **Fixation** | Methanol | 50.0 mL | |
| | Acetic acid | 12.0 mL | 2 hours/ |
| | Formaldehyde | 47.5 µL | Overnight |
| | Deionized water | Top up to 100.0 mL | |
| **Wash** | Ethanol (95%) | 35.0 mL | 3 x 20 minutes |
| | Deionized water | 65.0 mL | |
| **Sensitizing** | Sodium thiosulfate | 0.03 g | 3 minutes |
| | Deionized water | Top up to 100.0 mL | |
| **Wash** | Deionized water | | 3 x 5 minutes |
| **Silver reaction** | Silver nitrate | 0.2 g | |
| | Formaldehyde | 72.0 µL | 20 minutes |
| | Deionized water | Top up to 100 mL | |
| **Wash** | Deionized water | | 3 x 10 seconds |
| **Developing** | Sodium Carbonate | 6.0g | |
| | Formaldehyde | 47.25 mL | 3 – 5 minutes |
| | Sensitizing solution | 2.0 mL | |
| | Deionized water | Top up to 100.0 mL | |
| **Stop** | Methanol | 50.0 mL | |
| | Acetic acid | 12.0 mL | 5 minutes |
| | Deionized water | Top up to 100.0 mL | |
| **Reservation** | Acetic acid | 1.0 mL | |
| | Deionized water | 99.0 mL | |

To determine the pI of the purified protein, iso-electrofocusing was performed (Chee *et al.*, 2014).

### 3.5.3.2 Enzyme assay to determine substrate specificity of GST enzymes

GST activity with various substrates was assayed at room temperature in a model spectrophotometer (Habig *et al.*, 1981). Enzymatic assays with 1-chloro-2,4-nitrobenzene (CDNB), ethacrynic acid (EA), sulfobromophthalein (BSP), p-nitrobenzyl chloride (NBC) and trans-4-phenyl-3-butene-2-one (PBO) were determined in this studies.

The enzymatic reaction with ethacrynic acid (EA) was examined according to Habig *et al.* (1981). 2.8 ml 0.1 M sodium phosphate ($Na_3PO_4$) buffer after adjusted pH 6.5 were added with 50 µl of 15 mM GSH, 50 µl of 12 mM substrate, 100 µl of purified

protein sample were pipetted last into a 3 ml cuvette. The change of absorbance for EA is 270 nm. Molar absorption coefficient of EA is 5000 $M^{-1}cm^{-1}$.

The enzymatic reaction with p-nitrobenzyl chloride (NBC) was examined in a 3 ml cuvette of 2.6 ml 0.1 M sodium phosphate ($Na_3PO_4$) buffer with pH 6.5, 50 µl of 60 mM GSH, 50 µl of 60 mM substrate, and 100 µl of purified protein sample was added. The change of absorbance for NBC is 310 nm. Molar absorption coefficient of NBC is 1900 $M^{-1}cm^{-1}$.

The enzymatic reaction with 1-chloro-2,4-nitrobenzene (CDNB) and trans-2-octenal ($T_2O$) were conducted in a 3 ml cuvette of 2.8 ml 0.1 M sodium phosphate ($Na_3PO_4$) buffer with adjusted pH 6.5 consisting 50 µl of 60 mM GSH, 50 µl of 60 mM substrate, and 100 µl of purified protein sample. The change of absorbance for CDNB and $T_2O$ were measured at 340 nm and 225 nm respectively. Molar absorption coefficient of CDNB is 9600 $M^{-1}cm^{-1}$. Molar absorption coefficient of Trans-2-octenal is -22000 $M^{-1}cm^{-1}$. Molar absorption coefficient of Trans-2-octenal is -22000 $M^{-1}cm^{-1}$.

The enzymatic activities with trans-4-phenyl-3-butene-2-one (PBO) was conducted in a 3 ml cuvette of 2.8 ml 0.1 M sodium phosphate ($Na_3PO_4$) buffer with adjusted pH 6.5 containing consisting 50 µl of 15 mM GSH, 50 µl of 3 mM substrate, and 100 µl of purified protein sample. The change of absorbance for PBO is 290nm. Molar absorption coefficient of PBO is -24800 $M^{-1}cm^{-1}$.

The enzymatic activities with hexadienal and 2, 4-heptadienal were conducted in a 3 ml cuvette of 2.8 ml 0.1 M sodium phosphate ($Na_3PO_4$) buffer with adjusted pH 6.5 containing consisting 50 µl of 60 mM GSH, 50 µl of 3 mM substrate, and 100 µl of purified protein sample. The change of absorbance for hexadienal and 2, 4-heptadienal were measured at 280 nm. Molar absorption coefficient of hexadienal is -34200 $M^{-1}cm^{-1}$. Molar absorption coefficient of 2, 4-heptadienal is -30300 $M^{-1}cm^{-1}$.

Analysis of glutathione peroxidase action was performed by changing the technique carried by Di Ilio *et al.* (1986). The assay containing of 0.2 M of sodium phosphate ($Na_3PO_4$) with adjusted pH 7, 0.2 mM of GSH, 0.04 mM of NADPH, 0.1 µmol/min of glutathione reductase and 0.2 mM of hydrogen peroxide or cumene hydroperoxide and 100 µl of cleaned protein test. Changes of absorbance for each glutathione peroxidase movement was recorded at 366 nm. Molar retention coefficient of NADPH is -6220 $M^{-1}cm^{-1}$.

#### 3.5.3.3 Bioinformatic analysis of purified protein

Using bioinformatic techniques, GST sequences were identified in publicly accessible databases, and analysed to identify conserved amino acid residues. Multiple sequence alignment and phylogenetic analysis of the purified protein sample were carried out using Phyre2 software in order to study homology model, secondary structure and disorder prediction of the purified sample.

#### 3.5.3.4 LCMC/MS analysis

Protein bands were excised and transferred to a sterilized centrifuge tube before sending service provider. The analysis was carried out at Proteomics International Facility, located at Harry Perkins Institute of Medical Research, QEII Medical Centre, Nedlands, Perth, Australia.

Purified peptides were studied by tandem mass spectrometry, de novo sequenced followed by homology matched against known peptides in the Swiss-Prot protein database. Protein samples were firstly digested using 10mL trypsin digest solution (12.5 mg/mL trypsin, 25 mM ammonium bicarbonate) and incubated 24 hours at 377°. The digested peptides were then extracted by two 20-min incubations with 10– 20 mL ACN containing 1 % TFA (Bringans *et al.* Proteomics 2008). Peptides were analysed by

electrospray ionization mass spectrometry using the Agilent 1260 Infinity HPLC system coupled to an Agilent 6540 mass spectrometer. Tryptic peptides were loaded onto a C18 column 300 SB, 5 µm and separated with a linear gradient of water/ acetonitrile/ 0.1 % formic acid (v/v). Spectra were analysed to identify proteins of interest using Mascot sequence matching software with MSPnr100 database. Database: MSPnr100 Taxonomy: Bacteria (Eubacteria) (January 2016; 51,622,794 sequences) All Entries (January 2016; 75,925)

### 3.5.4 Bacterial sequencing identification

#### 3.5.4.1 Polymerization Chain Reaction (PCR)

A colony was picked from the culture plate and mixed well with 10 µL of sterilized distilled water in the small PCR tube. All the chemicals were thaw before use except for Taq polymerase. The master mix was prepared as below (Table 3.4):

**Table 3.4**: Preparation of Master mix.

| Promega | Concentration | Volume for 1 template (µL) |
|---|---|---|
| **Buffer** | X 5 | 10.0 |
| **$MgCl_2$** | 25 mM | 3.0 |
| **Primer (F)** | 5 µM | 2.0 |
| **Primer (R)** | 5 µM | 2.0 |
| **dNTPs** | 10 mM | 1.0 |
| **Taq polymerase** | 5 units | 0.1 |
| **Total** | - | 18.1 |

31.4 µL sterilized distilled water was pipetted into the sterilized tube followed by 18.1µL prepared mastermix (listed in Table 3.1) and 0.5 µL template. The primer in this research was 27F 1492R.

The sample was mixed well before proceeding to PCR. The reaction volume was set to 50 µL.

### 3.5.5.2 PCR protocol

The PCR protocol was set according to Table 3.5.

**Table 3.5**: PCR Protocol.

| **Initial Step** | **Each of 30 cycles** | | | **Final Extension** | **Final Step** |
|---|---|---|---|---|---|
| | Melt | Anneal | Extend | | |
| HOLD | CYCLE | | | HOLD | HOLD |
| 95ºC | 94ºC | 52.5ºC | 72ºC | 72ºC | 4ºC |
| 5 mins | 0.45 s | 0.30 s | 1.30 mins | 10 mins | ∞ |

### 3.5.5.3 Analysis of PCR products

5 µL of each of the sample was run on 1.5% (w/v) agarose gel. 2 µL of ladder was added with 2 µL of marker before loaded into the well. The gel electrophoresis was run for 20 minutes under 102 V. The gel was stained with ethidium bromide about 15 minutes and washed gently with distilled water then viewed under UV.

### 3.5.5.4 Gene sequencing

The 16s rRNA gene sequence was supported out by First Base laboratories Sdn. Bhd. The amplified nucleotide sequences were searched and blasted using NCBI database.

# CHAPTER 4: RESULTS

## 4.1 Protein Characterization

### 4.1.1 SDS-PAGE Analysis

The crude protein sample was purified using sulfobromothaphlein disodium salt-glutathione (BSP) affinity column, GSTrap™ affinity column and dinitrophenol-glutathione (DNP) affinity column respectively. After purified using each of the affinity chromatography respectively, each of the samples was collected and concentrated until 100 µl under 5000 rpm, 4 ºC. 10 µl of the concentrated purified sample was used to run SDS-PAGE. Figure 4.1 showing SDS PAGE of the purified protein from *Pseudomonas* sp. UW4 using BSP affinity column. The purified protein was made up of single subunit which had a molecular weight at about 17 kDa. From the Figure 4.1, the purified protein was appeared to be a homodimer made up of 17 k Da subunits.

From Figure 4.2 and Figure 4.3, we can conclude that both GSTrap™ affinity column and dinitrophenol-glutathione (DNP) affinity column could not purify the targeted protein well as there are many bands produced.

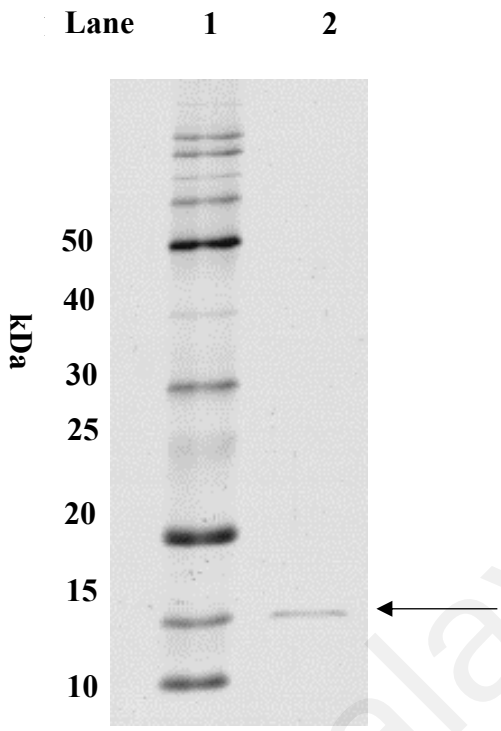


**Figure 4.1**: The SDS PAGE of purified protein from *Pseudomonas* sp. UW4 using sulfobromothaphlein disodium salt-glutathione (BSP) affinity column. First lane shows the BenchMark™ standard protein marker (Invitrogen brand), while arrow indicates the purified protein sample.

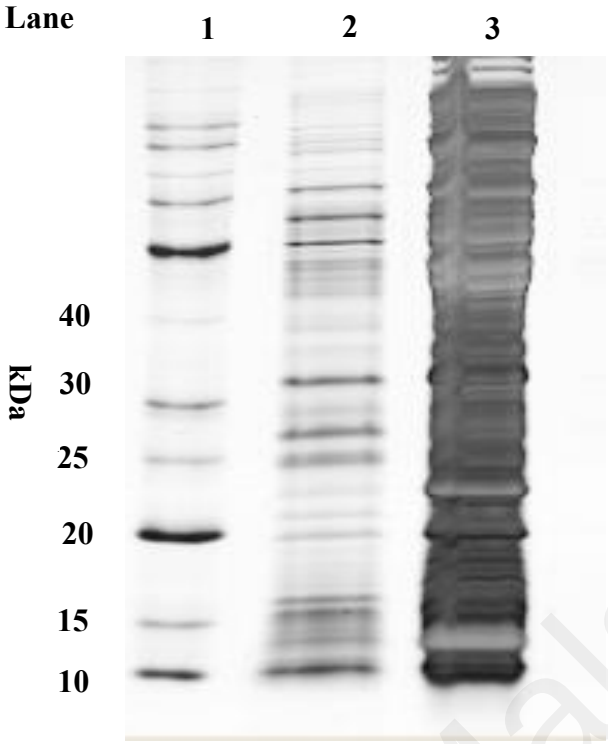


**Figure 4.2**: SDS PAGE of purified protein from *Pseudomonas* sp. UW4 using GSTrap™ affinity column. First lane indicates BenchMark™ standard marker (Invitrogen), second lane shows Purified protein sample and following lane is Crude protein.

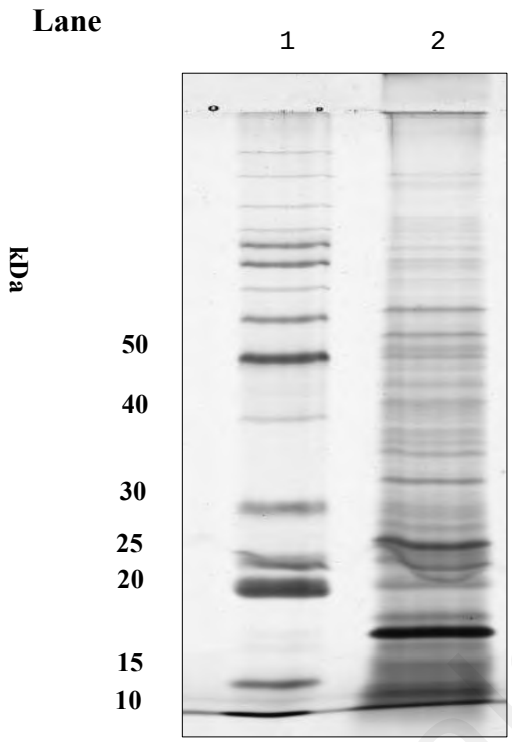


**Figure 4.3**: SDS PAGE of purified protein from *Pseudomonas* sp. UW4 using dinitrophenol glutathione (DNP) affinity column. First lane shows BenchMark$^{TM}$ standard marker (Invitrogen) and second lane indicates Purified protein sample.

### 4.1.2 Isoelectric focusing (IEF) of the purified protein

The purified protein from the *Pseudomonas* sp. UW4 was also performed a vertical isoelectric focusing gel to determine the pI value. Isoelectric-focusing of the purified protein resulted in one band at pI value of 6.1 (Figure 4.4).

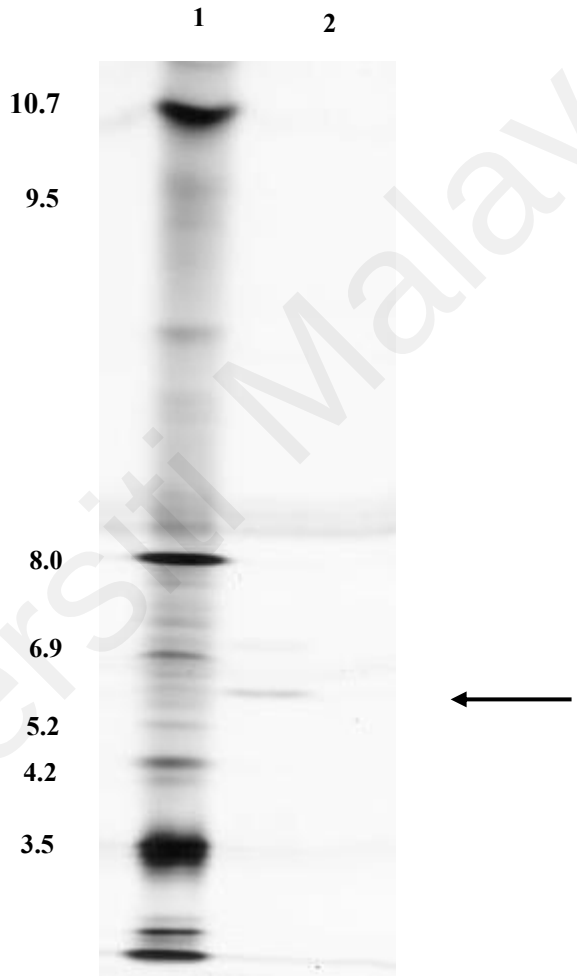


**Figure 4.4**: Isoelectric-focusing of purified GST (10 $\mu$g). First lane indicates the SERVA$^{TM}$ IEF marker (Invitrogen brand); Second lane indicates the pI value of the purified protein. Gel was stained with silver.

### 4.1.3 Substrate specificity test for the purified protein

Table 4.1 shows that the purified protein had a very significant value towards ethacrynic acid among the substrates stated in Table 4.1 and it also reacted with 1-chloro-2,4-dinitrobenzene which is a GST shared substrate. Besides that, the conjugation of the purified protein towards cumene hydroxide and hydrogen peroxide proposed the presence of glutathione peroxidase. However, it has no enzymatic activities with sulfobromopthalein, p-nitrophenyl chloride, 2,4-heptadienal, trans-2-octenal and trans-4-phenyl-3-butene-2-one. The result explained that it does not involve in lipid peroxidation because it has no enzymatic reaction with trans-2-octenal and trans-4-phenyl-3-butene-2-one.

**Table 4.1**: Substrate specificity of purified protein from *Pseudomonas* sp. UW4.

| **Substrate** | **GST** (nmol/min) |
|---|---|
| Ethacrynic acid | 291.62 ± 37.39 |
| 1-chloro-2,4-dinitrobenzene | 653.13 ± 17.04 |
| Cumene hydroperoxide | 430.86 ± 1.65 |
| Hydrogen peroxide | 52.42 ± 2.95 |
| 2,4-heptadienal | n.d |
| Trans-2-octenal | n.d |
| p-nitrophenyl chloride | n.d |
| Sulfobromopthalein | n.d |
| Trans-4-phenyl-3-butene-2-one | n.d |

Note: n.d : not detected

### 4.1.4 LCMS/MS analysis of purified protein

The band from one dimensional electrophoresis was excised and did not meet any similarities between other classes of GST found in *Pseudomonas* sp. UW4 or even GSTs from another bacteria species as well (Appendix F). The result cannot be established due to insufficient of protein concentration in the gel. Hence, more bacterial culture needed to obtain higher protein concentration. The top score was serum albumin

from Bos Taurus taxonomy. The score is too low and completely unrelated which the protein sequence coverage only 26%.

### 4.1.5 Characterization of GST from *Pseudomonas* sp. UW4

There are total 20 GSTs can be found in *Pseudomonas* sp. UW4 as shown in Table 4.2. In order to study the possible classes and relationship of each of the GSTs in *Pseudomonas* sp. UW4. A phylogenetic tree is constructed between 20 GSTs found in *Pseudomonas* sp. UW4 and some well-known established bacterial GSTs sequence (Figure 4.5). From Figure 4.5, it showed the relationship and the possible classes of all the glutathione found in *Pseudomonas sp.* UW4. There are few sista taxas can be found in the phylogenetic tree which suggested they have similar characteristics, for example PputUW4 02852 and PputUW 01628; PputUW4 01443 and PputUW 00801.

Besides that, from the Table 4.2, by comparing with the molecular weight and pI value which have found in this research, Ppuw4_00801 is chosen as its molecular weight, pI value and characteristics was close and very similar to the result obtain from the finding. The possible 3D model was studied using Phyre2 software (Figure 4.7). The complete protein gene sequence can be obtained from the *Pseudomonas* database as shown in Figure 4.6. The 3D model of Ppuw4_00801 was studied using its complete protein gene sequence (Figure 4.8).

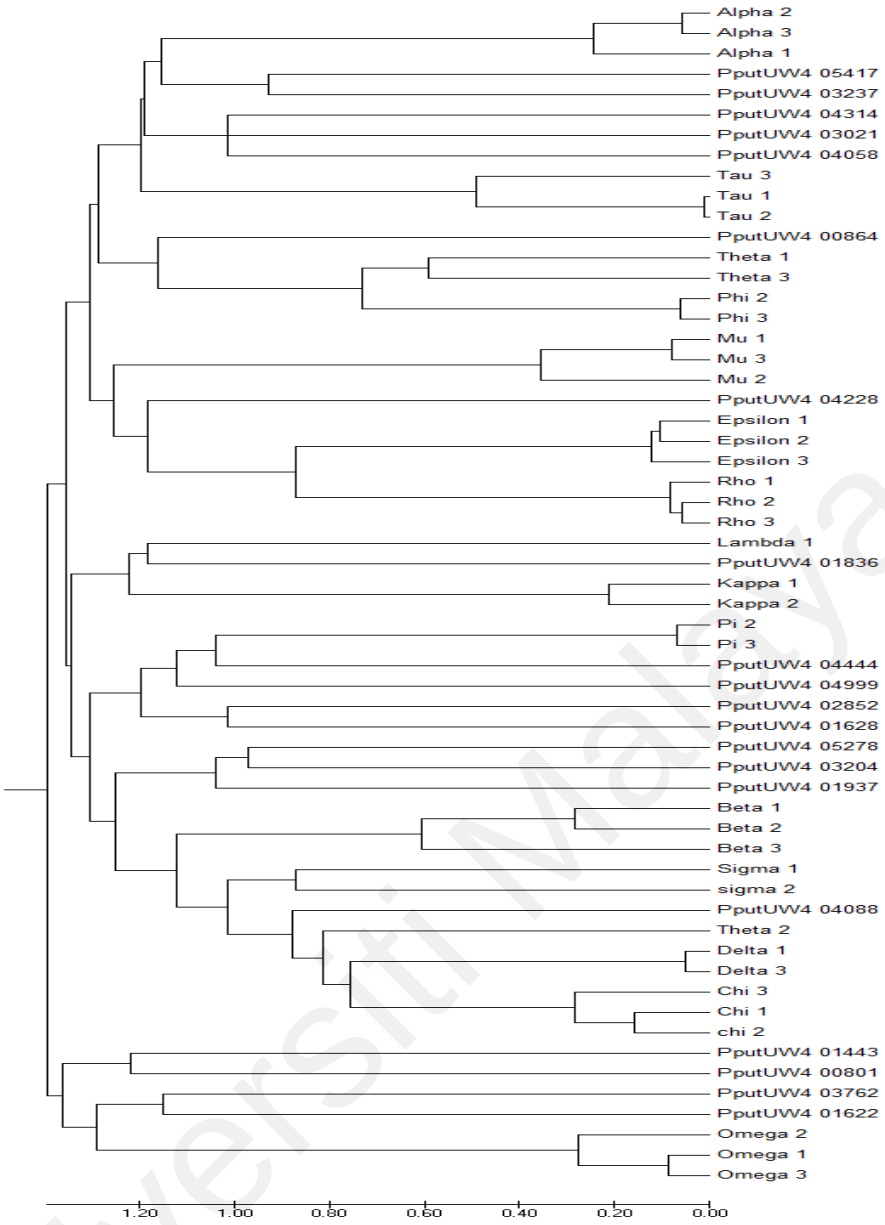


**Figure 4.5**: Evolutionary relationships of taxa for all the glutathione found in *Pseudomonas* sp. UW4. The evolutionary history was inferred using the UPGMA method and the optimal tree with the sum of branch length = 45.85461386 is shown. The tree is drawn to scale, with branch lengths in the same units as those of the evolutionary distances used to infer the phylogenetic tree. The evolutionary distances were computed using the Poisson correction method and are in the units of the number of amino acid substitutions per site. The analysis involved 68 amino acid sequences. All positions containing gaps and missing data were eliminated. There were a total of 158 positions in the final dataset. Evolutionary analyses were conducted in MEGA7 software.

**Table 4.2**: All the putative glutathione transferases found in *Pseudomonas* sp. UW4.

| No. | **Locus Tag** | **Gene** | **Molecular Weight (kDa)** | **Isoelectric Point (pI)** |
|---|---|---|---|---|
| 1 | PputUW4_04444 | Glutathione S-Transferase | 34.06 | 6.05 |
| 2 | PputUW4_01622 | Glutathione S-Transferase | 26.73 | 5.39 |
| 3 | PputUW4_01836 | Glutathione S-Transferase | 38.24 | 6.65 |
| 4 | PputUW4_05417 | Glutathione S-Transferase | 22.48 | 6.52 |
| 5 | PputUW4_03237 | Glutathione S-Transferase | 2.72 | 7.92 |
| 6 | PputUW4_04058 | Glutathione S-Transferase | 23.24 | 5.31 |
| 7 | PputUW4_04228 | Glutathione S-Transferase | 24.36 | 6.91 |
| 8 | PputUW4_04088 | Glutathione S-Transferase | 24.51 | 6.80 |
| 9 | PputUW4_04314 | Glutathione S-Transferase | 23.22 | 6.52 |
| 10 | PputUW4_04999 | Glutathione S-Transferase | 24.70 | 5.30 |
| 11 | PputUW4_05278 | Glutathione S-Transferase | 23.94 | 5.76 |
| 12 | PputUW4_01937 | Glutathione S-Transferase | 22.37 | 4.56 |
| 13 | PputUW4_03021 | Glutathione S-Transferase | 25.38 | 6.60 |
| 14 | PputUW4_03204 | Glutathione S-Transferase | 25.20 | 6.93 |
| 15 | PputUW4_01628 | GST-like protein | 23.11 | 6.30 |
| 16 | PputUW4_02852 | GST-like protein | 23.07 | 5.38 |
| 17 | PputUW4_00864 | GST-like protein | 24.33 | 6.68 |
| 18 | PputUW4_03762 | Glutathione S-Transferase (Glutathione Peroxidase) | 20.61 | 8.19 |
| 19 | PputUW4_00801 | Glutathione S-Transferase (Glutathione Peroxidase) | 17.60 | 6.10 |
| 20 | PputUW4_01443 | Glutathione S-Transferase (Glutathione Peroxidase) | 17.60 | 9.27 |

Among all the 3D homologues, the ppuW4_00801 has 38 % similar identity with template c2v1mA under 100% confidence level with 98 % coverage (Figure 4.7). The first ‘c’ indicates this protein is a whole chain taken from PDB with PDB identifier 2v1m and chain identifier A. 2v1m is a *Schistosoma mansoni* glutathione peroxidase which also have the same classification as oxidoreductase (Dimastrogiovanni *et al.*, 2009).

MSAFHDLKLTALDGQELPLAPFKGQVVLVVNVASKCGLTPQYAALENLYQQ

YKAKGFSVLGLPCNQFAGQEPGTEQEIKDFCSLNYGVTFPLSSKLEVNGHDR

HQLYRLLAGEGAEFPGDITWNFEKFLLGKDGRVLARFSPRTAPDDPTIVHAIE

**Figure 4.6**: ppuW4 00801 complete protein gene sequence.

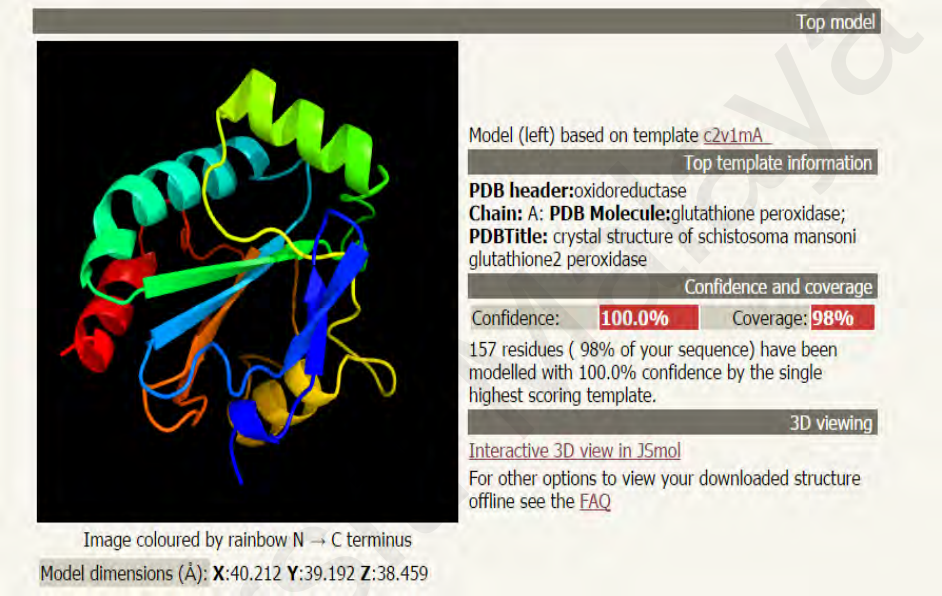


**Figure 4.7**: The homologous model for Ppuw4_00801 obtained from Phyre2 software.

**Figure 4.8**: The homology structure of Ppuw4_00801 obtained from Phyre2 software.

The position in the amino acid sequence are shown in the first and second line (Figure 4.9). The amino acid residues are coloured based on chracteristics properties whether small, polar (orange), or hydrophobic (green), or charged (red) or aromatic and cysteine (blue). On the third line is the prediction of the secondary structure which consists of alpha helix (green), beta strand (blue arrows) and coil (faint lines). The 'SS confidence' showed most of the prediction in this structures were high which were marked in red. However, there are some parts between of the structures has low confidence which was indicated with orange, yellow and green colors. Next, there are some question marks (?) found in the disorder line which are the prediction of disordered region in ppUW_00801. The disordered region in helix prediction indicated the parts where consist of important functionalities.

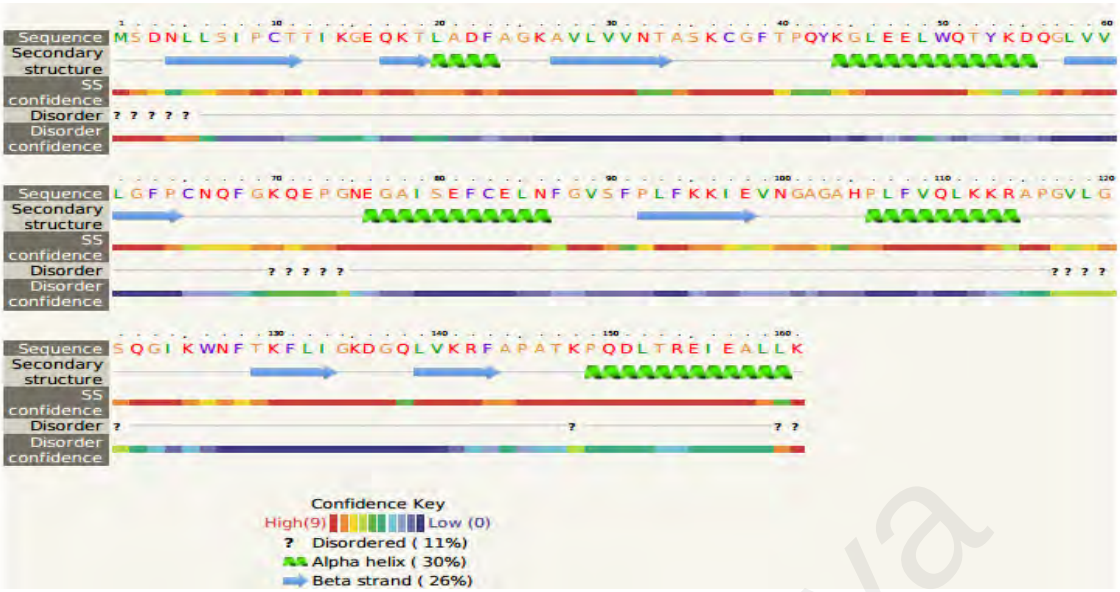


**Figure 4.9**: Secondary structure and disorder prediction for Ppuw4_00801.

# CHAPTER 5: DISCUSSION

The genus *Pseudomonas* consist different types of species carries diverse functions of ecological, economic, and health-related importance. Some species are pathogenic for plants, animals or humans. However, there are some species serve as good bacteria, known as rhizosphere, exhibiting plant growth-promoting and pathogen-suppressing functions and may be exploited for use in biological control. These metabolic versatile are valued in biotechnology and bioremediation. Therefore, by studying and exploring *Pseudomonas* sp. in the environment help us to have more understanding of the ecological significance of these microorganisms. To date, a lot of studies have proven that *Pseudomonas* sp. can degrade a variety of compounds.

The plant growth-promoting bacteria (PGPB) *Pseudomonas* sp. UW4 was obtained and isolated from the rhizosphere of common reeds growing on the campus of the University of Waterloo. This species promotes plant growth in the presence of different environmental stresses. This project serves as a preliminary study of isolating and studying the characteristic of glutathione transferases in the bacteria.

The complete genome sequence of the *Pseudomonas* sp. UW4 was only established at year 2013 which was still novel and it is characterized under *Pseudomonas fluorescence* group, *jessenii* subgroup (Figure 5.1). There are 20 different types of glutathione transferases can be found in *Pseudomonas* sp. UW4 (Table 4.2). Phylogenetic trees is constructed using molecular evolution genetics analysis (MEGA software). By studying the phylogenetic trees, they are hardly been classified respectively as they did not under known GST classes (Figure 4.5). They are branched, grouped together and formed sister taxa or polytomy where the relationships in between are not clearly shown even though they branched out from the same ancestor.

The utilization of 16s rRNA arrangements can be utilized to investigate bacterial phylogeny and categorization. This was a general and broad utilized strategy as it is a viable and quick way; the 16s rRNA quality found in the greater part of the microscopic organisms either as a multigene family, or operons; the capacity of the 16S rRNA quality after some time has not changed, proposing that irregular arrangement varieties are a more precise measure of time; and the 16S rRNA quality (1,500 bp) is adequate for informatics judgments (Sujatha *et al.*, 2012). In any case, utilizing 16s rRNA groupings not an edit and indisputable for some of circumstance for instance 16 rRNA can't give a complete answer and recognize as of late wandered species or the contrast between the nearest and next nearest match to the example have 99.5% comparability which just have is 0.5% difference.

A single colony of *Pseudomonas* sp. UW4 on the tryptic soy agar was picked, followed by PCR amplification of 16S rRNA. Comparing with the Kplus DNA ladder, the thick single band has 1500 base pair which indicated that total base pair in 16S rRNA of the bacterial strain. After blasted with the sequence obtained, most of the strains given in the NCBI were under *Pseudomonas fluorescens* group. *Pseudomonas* sp. UW4 showed 99% sequence similarity with *Pseudomonas fluorescens* sp. (Figure 5.2).

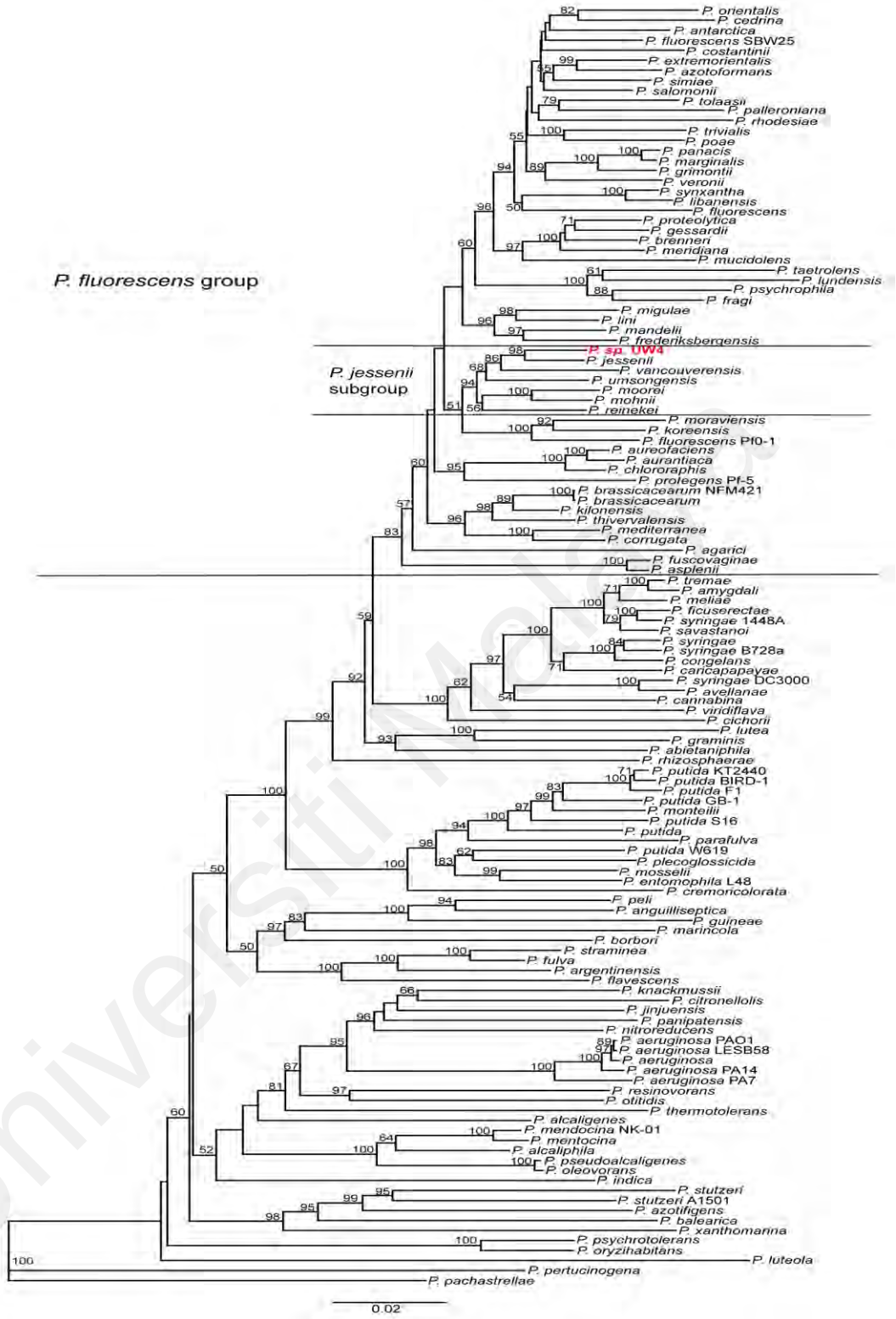


**Figure 5.1**: Phylogenetic tree of 128 Pseudomonas strains created on four concatenated genes (16S rRNA, gyrB, rpoB and rpoD). Dendrogram was studied by neighbor-joining. The bar at the bottom indicates sequence divergence and distance matrix was calculated by the Jukes-Cantor algorithm. Nodal support was assessed with 1000 bootstrap pseudoreplications and figures of more than 50% are revealed at the nodes (Duan *et al.*, 2013).

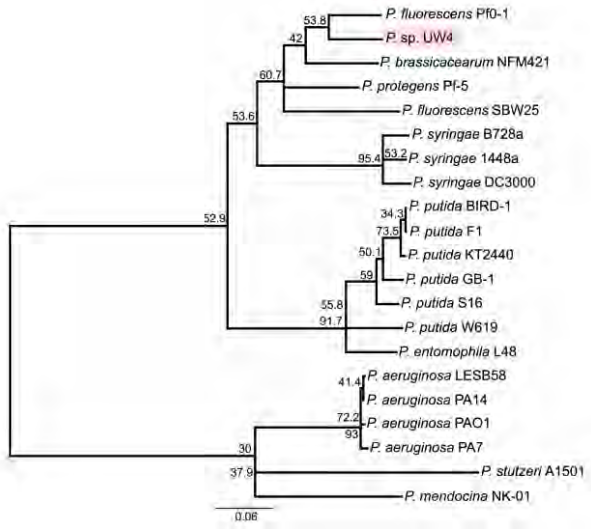


**Figure 5.2**: Phylogenetic tree of 21 different Pseudomonas species that replied on 1,679 conserved genes. Numbers on nodes represent percentages of individual trees containing that relationship and the scale bar corresponds to the number of substitutions per site (Duan *et al.*, 2013).

The putative GST from *Pseudomonas sp.* UW4 was purified from cell lysate using affinity chromatography on a glutathione BSP-agarose column and one about 17kDa band is shown on SDS-PAGE gel. Sulfobromophthalein-glutathione conjugate (BSP) was immobilized to an agarose matrix by using either cyanogen bromide or epichlorohydrin activation and commonly used to purify GST from sample such as *Galleria mellonella*, *Costelytra zealandica*, *Musca domestica*, *Drosophila melanogaster* and *Wiseana cervinata* (Clark *et al.*, 1967; Clark *et al.*, 1984; Clark *et al.*, 1990). Another form of affinity matrix that has been used widely is the immobilized GSH-agarose matrix which has been used to purify GSTs from a few insects. However, it did not applicable for *Pseudomonas sp.* UW4 sample. Many bands found on SDS-PAGE gels after purified the sample using affinity chromatography on a immobilized GSH-agarose matrix. This has indicated that GST expressing protein only can be purified using glutathione BSP-agarose column.

Among all the substrates, purified putative GST had a very significant affinity towards ethacrynic acid. According to early studies, this behavior is similar to a Pi (π) class GSTs (Wongtrakul *et al.*, 2012) as Pi class was characterized by EA substrate specificity. Reactivity with ethacrynic acid (EA) showed the ability of the purified putative GST involve in the biochemical reaction of alkylating drugs towards drug resistant cells (Simarani *et al.*, 2016). The purified putative GST has low activity towards 1-chloro-2,4-dinitrobenzene (CDNB) which is a recognised substrate for GSTs from other organisms especially for beta class GST. The low activity with this substrate is in line with bacterial GSTs (Zablotowicz *et al.*, 1995). The ability of the enzyme to conjugate EA and DCNB suggested the presence of pi and mu class GSTs (Arakawa *et al.*, 2012) in the bacterial enzyme.

Our study showed that purified putative GST reacted with both hydrogen peroxide and cumene hydroperoxide, thus showing selenium-independent glutathione peroxidase activity. Glutathione peroxidase catalyse the reduction of hydrogen peroxide and organic hydroperoxides to water or the corresponding alcohols using reduced glutathione as electron donor.

$$ROOH + 2GSH \rightarrow ROH + H_2O + GSSR$$

However, the purified putative GST has no activity with trans-octenal, hepta 2,4 dienal, and trans-4-phenyl-3-butene-2-one, indicating purified putative GST was not involved in lipid peroxidation (Lilian *et al.*, 2016). The activities of purified putative GST towards substrates were not significant which might due to the eluates containing salt (NaCl). GST protein in the eluate would denatured or contorted by the ionic interaction because of the sodium chloride salt found in reaction (Date *et al.*, 2013). Protein stability can be influenced by the grouping of salt in the reaction. Electrostatic

impacts on self-polarization energy and cross-polarization energy, or screening of electrostatic attraction may be one of the variables. The second factors affect the protein stability is the solute-solvent interface with an increasing of concentration of salt (Date *et al.*, 2013). The salt would have interaction to the R groups side chain of amino acid thus disrupt the ionic salt bonding or electrostatic relations that are stabilized both tertiary and quaternary level.

Purified putative GST isozymes in *Pseudomonas* sp. UW4 was analysed by using isoelectric-focusing (IEF) gel and can be purified using affinity chromatography on a glutathione BSP-agarose column. Isoelectric-focusing of the purified sample resulted in one band at pI value of about 6.1 which is slightly acidic (Figure 4.4). This has suggested that acidic groups of amino acids in the purified protein slightly more than basic groups. At this point, it has no electrical net charge and stop migrate. Thus, the proteins become focused into sharp stationary bands with each protein positioned at a point in the pH gradient corresponding to its pI.

LCMS/MS analysis of the purified putative GST had been identified as Serum albumin from *Bos taurus* and Serum albumin from *Ovis aries*. LCMS/MS analysis unable to significantly identify the purified putative GST as a family of bacterial glutathione transferase or any other proteins from *Pseudomonas* sp. However, among the total 20 putative glutathione transferases of *Pseudomonas* sp. UW4 information obtained from *Pseudomonas* database, ppUW4_00801 have closest characteristics and properties to purified putative GST. A phylogenetic tree was constructed between the total 20 putative glutathione transferases of this strain with different classes of known glutathione transferases (Figure 4.5). It shows that ppUW4_00801 located close to Omega class glutathione transferase. Up to date, there is rare bacteria GSTs can be found under Omega class, suggesting that it would be a new class of GST.

By comparing with the molecular weight and pI value of the purified putative GST, Ppuw4_00801 is chosen as its molecular weight and pI value was close to the result obtain from the finding (Table 4.2). The coding profiles and the homology patterns were analyzed using Phyre2 software. By submitting the gene sequence, the sequence homologues were compared and analysed with PSI-Blast, both secondary structure and disorder with Psi-pred and Diso-pred predicted then a hidden Markov model model (HMM) of the requested sequence was constructed based on the homologues detected. After that, a set of potential 3D models produced based on alignment between the HMM of the requested sequence to known protein structure.

Among all the 3D homologues, the ppuW4 00801 has 38% similar identity with template c2v1mA under 100% confidence level with 98% coverage. The proposed model consists of above 30-40% similarity. The first 'c' indicates this protein is a whole chain taken from Protein Data Bank (PDB) with PDB identifier 2v1m and chain identifier A. 2v1m is a *Schistosoma mansoni* glutathione peroxidase which also have the same classification as oxidoreductase (Dimastrogiovanni *et al.*, 2009). In this paper, 2v1m serves as a sulfur or selenium dependent isoenzymes and can reduces peroxides using the reducing equivalents provided by glutathione or thioredoxin. Besides that, by analysing cysteine and serine residues using static crystallography with molecular dynamics simulations, both residues serve a role for the catalytic activity. The presence of glutathione peroxidase in the *Schistosoma mansoni* serve as antioxidant enzymes that inhibit by degradation of the reactive oxygen produced by the host's innate response. Thus, glutathione peroxidase serves as a potential target for the development of drugs or vaccine against Schistosomiasis (Song *et al.*, 2012; Gendy *et al.*, 2013).

The result below (Figure 5.3) shows most of the alignment between query (protein structure of P puw_00801) and the template (crystal structure of *Schistosoma mansoni* glutathione peroxidase, c2v1mA) matched well. Therefore, the homologue structure predicted for Ppuw_00801 is reliable.

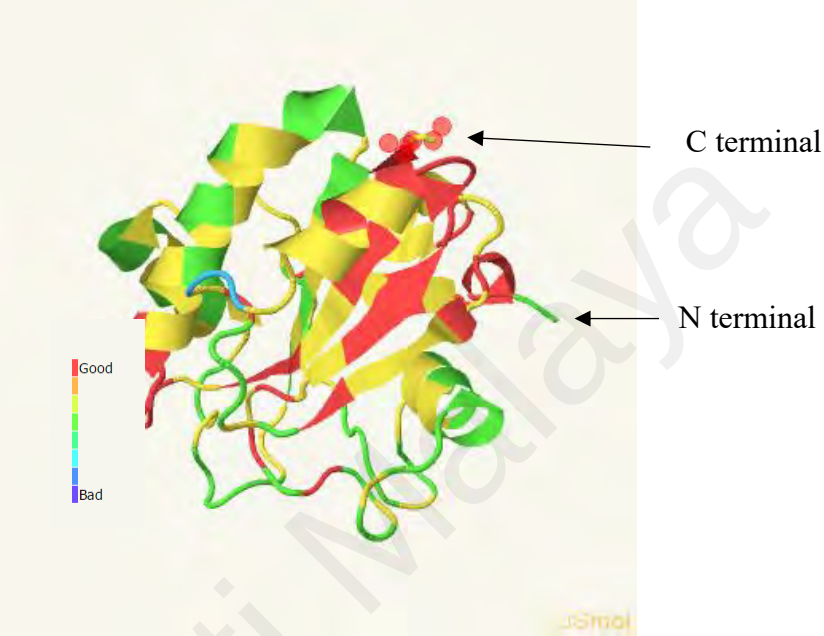


**Figure 5.3**: Alignment confidence of the pairwise query-template alignment as reported by HHsearch. The confidence values are obtained from the posterior probabilities calculated in the Forward-Backward algorithm.

# CHAPTER 6: CONCLUSION

Glutathione transferases (GSTs) was extracted and purified from *Pseudomonas* sp. UW4 obtained from University of Waterloo, Canada using affinity chromatography. Three different glutathione-affinity chromatography which are GSTrap$^{TM}$, dinitrophenol-glutathione (DNP) column and BSP column were applied respectively to purify the GSTs from the *Pseudomonas* sp. UW4. However, SDS-polyacrylamide gel electrophoresis revealed that the GSTs only can be purified from crude protein using BSP column. The purified GST purified resolved into a single band with low molecular weight (MW) of 17 kDa. Isoselectrofocusing showed it exists in single band with pI 6.1.

The purified putative GSTs was characterized and identified through bioinformatic analysis and their substrate specificities. Based on the substrate specificity test, the purified putative GST was reactive towards ethacrynic acid (EA) (2.9162 ± 0.03739µmol/min), CDNB (0.653125 ± 0.01704 µmol/min), cumene hydroxide (0.430862 ± 0.00165µmol/min) and hydrogen peroxide (0.052423 ± 0.00295µmol/min), but no conjugation activity towards trans-2-octenal, hepta-2,4-dienal and trans-4-phenyl-3-butene-2-one. This demonstrated that putative GST possessed peroxidase activity but is not involved in lipid peroxidation. The purified GST suggested to be similar to PputUW4_00801 (putative glutathione S-transferase) of *Pseudomonas* sp. UW4.

An attempt to identify the purified putative GSTs by LCMS/MS analysis were futile as it incompetent to produce agreeably consistent outcomes and generated inconsistent results on sample in this studies. However our other studies have supported the finding. The utmost evidence was the binding to sulfobromopthalein glutathione-affinity chromatography during purification from the crude protein. Furthermore, the purified putative GSTs did conjugate with GST common substrates which are EA and CDNB. Based on our finding, the putative GSTs had hydroperoxidase activity.

As compared to all the characteristics observed in our finding between the GSTs of *Pseudomonas* sp. UW4 obtained from the *Pseudomonas* database, ppUW4_00801 (glutathione peroxidase) have similar characteristics and properties to purified putative GSTs. A phylogenetic tree was also constructed between the purified putative GSTs and known GSTs, unfortunately the purified putative GSTs unable to be classified reliably as it has showed that ppUW4_00801 located close to Omega class GST.

The possible 3D model of ppUW4_00801 was studied using Phyre2 software and it revealed 38% similar identity with *Schistosoma mansoni* glutathione peroxidase under 100% confidence level with 98% coverage. The following proof was both have the similar characteristics as they are glutathione peroxidase.

## REFERENCES


Allocati, N., Federici, L., Masulli, M., & Di Ilio, C. (2009). Glutathione transferases in bacteria. *FEBS Journal*, *276*(1), 58–75.

Allocati, N., Masulli, M., Casalone, E., Santucci, S., Favaloro, B., Parker, M. W., & Di Ilio, C. (2002). Glutamic acid 65 is an essential residue for catalysis in *Proteus mirabilis* glutathione S-transferase B1-1. *Biochemical Journal*, *363*, 189–193.

Anandarajah, K., Kiefer, P. M. J., Donohoe, B. S., & Copley, S. D. (2001). Recruitment of double bond isomerase to serve a reductive dehalogenase during biodegradation of pentachlorophenol. *Biochemistry Journal*, *39*(18), 5303-5311.

Angelucci, F., Dimastrogiovanni, D., Boumis, G., Brunori, M., Miele, A. E., Saccoccia, F., & Bellelli, A. (2010). Mapping the catalytic cycle of *Schistosoma mansoni* thioredoxin glutathione reductase by X-ray crystallography. *Journal of Biological Chemistry*, *285*(42), 32557-32567.

Arakawa, S., Maejima, T., Kiyosawa, N., Yamaguchi, T., Shibaya, Y., Aida, Y., … Takasaki, W. (2012). Methemoglobinemia induced by 1,2-dichloro-4-nitrobenzene in mice with a disrupted glutathione S-transferase mu 1 gene. *The American Society for Pharmacology and Experimental Therapeutics*, *38*, 1545-1552.

Booth, J., Boyland, & E., Sims, P. (1961). An enzyme from rat liver catalyzing conjugations with glutathione. *Biochemical Journal*, *79*(3), 516-522.

Boumis, G., Angelucci, F., Bellelli, A., Brunori, M., Dimastrogiovanni, D., & Miele, A. E. (2011). Structural and functional characterization of *Schistosoma mansoni* Thioredoxin. *Protein Science*, *20*, 1069-1076.

Bryan, AB., & Richard, NA. (2001). Elementary Steps in the Acquisition of $Mn^{2+}$ by the Fosfomycin Resistance Protein (FosA). *Biochemistry*, *40*(42), 12712–12718.

Castaneda, A. G., Blazquez, J., & Rodriguez, R. (2013). Molecular Mechanisms and Clinical Impact of Acquired and Intrinsic Fosfomycin Resistance. *Antibiotics*, *2*, 217-236.

Chee, C. S., Tan, I. K. P., & Alias, Z. (2014). Characterization of Affinity-Purified Isoforms of *Acinetobacter calcoaceticus* Y1 Glutathione Transferases. *The Scientific World Journal*, *10*(4), 215-221.

Cheng, Z. Y., Wei, Y. Y. C., Sung, W. W. L., Glick, B. R., & McConkey, B. J. (2009). Proteomic analysis of the response of the plant growth-promoting bacterium Pseudomonas putida UW4 to nickel stress. *Proteome Science*, *7*(18), doi: 10.1186/1477-5956-7-18.

Clark, A. G., Darby, F., & Smith, J. N. (1967). Species difference in the inhibition of glutathione s aryltransferase by phthaleins and dicarboxylic acids. *Biochemistry Journal*, *103*, 49-54.

Clark, A. G., Marshall, S. N., & Qureshi, A. R. (1990). Synthesis and use of an isoform-specific affinity matrix in the purification of glutathione *S*-transferases from the housefly, *Musca domestica. Protein Expression and Purification, 1*(2), 121-126.

Clark, A. G., Sharmaan, N. A., Dauterman, W. C., & Hayaoka, T. (1984). Characterization of multiple glutathione transferases from the house fly, *Musca Domestica*. *Pesticide Biochemistry and Physiology*, *22*(1), 51-59.

Date, M. S., & Dominy, B. N. (2013). Modelling the influence of salt on the hydrophobic effect and protein fold stability. *Communications in Computational Physics*, *13*(1), 90-106.

Dimastrogiovanni, D., Anselmi, M., Meile, A. E., Boumis, G., Petersson, L., Angelucci, F., … Bellelli, A. (2009). Combining crystallography and molecular dynamics: The case of *Schistosoma mansoni* phospholipid glutathione peroxidase. *Protein: Structure, Function, and Bioinformatics*, *78*(2), 259-270.

Di Ilio, C., Sacchetta, P., Bello, M. L., Caccuri, A. M., & Federici, G. (1986). Selenium independent glutathione peroxidase activity associated with cationic forms of glutathione transferase in human heart. *Journal of Molecular and Cellular Cardiology*, *18*(9), 983-991.

Duan, J., Jiang, W., Cheng, Z. Y., Heikkila, J. J., & Glick, B. R. (2013). The complete genome sequence of the plant growth promoting bacterium *Pseudomonas* sp. UW4. *PLoS ONE*, *8*(3), 1-19.

Duca, D., Rose, D. R., & Glick, B. R. (2014). Characterization of a nitrilase and a nitrile hydratase from *Pseudomonas* sp. UW4 that converts indole-3-acetonitrile to produce indole-3-acetic acid. *Applied and Environmental Microbiology*, *80*(15), 4640-4649.

Favaloro B., Melino S., Petruzzelli R., Di Ilio, C., & Rotilio, D. (1998). Purification and characterization of a novel glutathione transferase from *Ochrobactrum anthropi*. *FEMS Microbiology Reviews*, *160*, 81–86.

Fillgrove, K. L., Pakhomova, S., Schaab, M. R., Newcomer, M. E., & Armstrong, R. N. (2007). Structure and mechanism of the genomically encoded fosfomycin resistance protein, fosX, from *Listeria monocytogenes*. *Biochemistry*, *46*(27), 8110–8120.

Geisla, M. S. S., Luciene, C. F., Marcelo, F., Sheila, C. C., Poliana, M. D., & Magda, F. (2012). Mechanisms of action of systemic antibiotics used in periodontal treatment and mechanisms of bacterial resistance to these drugs. *Journal of Applied Oral Science*, *20*(3), 295-309.

Gendy, A. E., Rabie, I., Deeb S. E., & Amir, A. M. E. (2013). Importance of *Schistosoma mansoni* thioredoxin reductase: 1-evaluation of its role in Schistosomiasis Diagnosis in Human. *Journal of Medical Sciences*, *13*(8), 635-646.

Habig, W. H., & Jakoby, W. B. (1981). Assays for differentiation of glutathione S-Tranferases. *Methods in Enzymology*, *77*, 398-405.

Hofer, B., Backhaus, S., & Timmis, K. N. (1994). The biphenyl/polychlorinated biphenyl-degradation locus (bph) of *Pseudomonas* sp. LB400 encodes four additional metabolic enzymes. *Gene*, *144*(1), 9–16.

Karageorgopoulos, D. E., Wang, R., Yu, X. H., & Falagas, M. E. (2011). Fosfomycin: evaluation of the published evidence on the emergence of antimicrobial resistance in Gram-negative pathogens. *Journal of Antimicrobial Chemotherapy, 67*, 255–268.

Kurabayashi, K., Hirakawa, Y., Tanimoto, K., Tomita, H., & Hirakawa, H. (2014). Role of the CpxAR Two-Component Signal Transduction System in Control of Fosfomycin Resistance and Carbon Substrate Uptake. *Journal of Bacteriology*, *196*(2), 248-25.

Lilian, P. P., Luiz, R. O., Leandro, D. T., Bruno, C. E. S., Pericles, M. R., Paula, F. M., … Marcos, P. (2016). GST activity and membrane lipid saturation prevents mesotrione-induced cellular damage in *Pantoea ananatis*. *AMB Express*, *6*(1), doi: 10.1186/s13568-016-0240-x.

Mannervik, B., Alin, P., Guthenberg, C., Jensson, H., Tahir, M. K., Warholm, M., & Jornwall, H. (1985). Identification of three classes of cytosolic glutathione transferase common to several mammal species: Correlation between structural data and enzymatic properties. *Biochemistry*, *82*, 7202-7206.

Nebert, D. W., & Vasillou, V. (2004). Analysis of the glutathione S-transferase (GST) gene family. *Human Genomics*, *1*(6), 460-464.

Nikolaidis, I., Favini, S. S., & Dessen, A. (2014). Resistance to antibiotics targeted to the bacterial cell wall. *Protein Science*, *23*(3), 243-259.

Nishida, M., Harada, S., Noguchi, S., Satow, Y., Inoue, H., & Takahashi, K. (1998). Three-dimensional structure of Escherichia coli glutathione S-transferase complexed with glutathione sulfonate: catalytic roles of Cys10 and His106. *Journal of Molecular Biology*, *281*(1), 135–147.

Oakley, A. J. (2011). Glutathione transferases: A structural perspective. *Drug Metabolism Reviews*, *43*(2), 138-151.

Pandey, T., Singh, S. K., Chhetri, G., Tripathi, T., & Singh, A. K. (2015). Characterization of a Highly pH Stable Chi-Class Glutathione S-Transferase from *Synechocystis* PCC 6803. *PLoS ONE*, *10*(5), Article #e0126811.

Pasiar, M., Rouhi, L., Bamzadeh, Z., & Hejazi, S. H. (2016). Invitro selective growth inhibition of breast adenocarcinoma cell lines by *Pseudomonas* sp. UW4 metabolites. *Tehran University Medical Journal*, *74*(9), 614-620.

Rigsby, R. P. (2005). *Studies of Genomic Fosfomycin Resistance Protein from Pseudomonas Aeruginosa* (Doctoral dissertation, Vanderbilt University). Retrieved on September 24, 2019 from https://etd.library.vanderbilt.edu//available/etd-06282005-084134.

Rui, L. Y., Kwon, Y. M., Reardon, K. F., & Wood, T. K. (2004). Metabolic pathway engineering to enhance aerobic degradation of chlorinated ethenes and to reduce their toxicity by cloning a novel glutathione *S*-transferase, an evolved toluene *o*-monooxygenase, and γ-glutamylcysteine synthetase. *Environmental Microbiology*, *6*(5), 491-500.

Shahniani, A., Birgani, PA., & Shirali, M. (2017). Effect of *Pseudomonas* sp. UW4 native strain metabolites on HT29 cell line proliferation and apoptosis. *Specialty Journal of Medical Research and Health Sciences*, *2*(4), 44-53.

Sheehan, D., Meade, G., Foley, V. M., & Dowd, C. A. (2001). Structure, function and evolution of glutathione transferases: implications for classification of non-mammalian members of an ancient enzyme superfamily. *Biochemical Journal*, *360*(1), 1-16.

Sheratt, P. J., & Hayes, J., D. (2001). Glutathione S-transferases. *Enzyme Systems that Metabolise Drugs and Other Xenobiotics*. Edited by Costas Ioannides, Copyright John Wiley & Sons Ltd. University of Dundee, UK.

Shi, Y. L., Wang, Q. F., Hou, Y. H., Hong, Y. Y., Xiao, H., Yi, J. L., Qu, J. J., & Lu, Y. (2014). Molecular cloning, expression and enzymatic characterization of glutathione S-transferase from Antarctic sea-ice bacteria *Pseudomonas* sp. ANT506. *Microbiological Research*, *160*, 179-184.

Simatani, K., Haizatul, WACY., & Alias, Z. (2016). Purification of glutathione transferases (GSTs) from identified rhizospheric bacteria. *Sains Malaysiana*, *45*(7), 1057-1062.

Skopelitou, K., Dhavala, P., Papageorgiou, AC., & Labrou, NE. (2012). A Glutathione Transferase from Agrobacterium tumefaciens Reveals a novel class of bacterial GST superfamily. *PLoS ONE 7*(4), Article #e34263.

Song, L. J., Li, J. H., Xie, S. Y., Qian, C. Y., Wang, J., Zhang, W., … Yu, C. X. (2012). Thioredoxin gluthione reductase as a novel drug target: Evidence from *Schistosoma japonicum*. *PLoS ONE*, 7(2), Article #e31456.

Sujatha, P., Kumar, B. N., & Kalarani, V. (2012). Isolation, characterization and molecular identification of bacteria from tannery effluent using 16SrRNA sequencing. *Current Biotica*, *6*(2), 198-207.

Thompson, M. K., Keithly, M. E., Goodman, M. C., Hammer, N. D., Cook, P. D., Jagessar, K. L., … Armstrong, R. N. (2014). Structure and function of the genomically encoded fosfomycin resistance enzyme, FosB, from *Staphylococcus aureus*. *Biochemistry*, *53*, 755-765.

Vuilleumier, S. (1997). Bacterial Glutathione S-transferases: What Are They Good for? *Journal of Bacteriology*, *179*(5), 1431-1441.

Winayanuwattikum, P., & Ketterman, A. J. (2005). An electron-sharing network involved in the catalytic mechanisms is functionally conserved in different glutathione transferase classes. *The American Society for Biochemistry and Molecular Biology*, *280*(3), 31776-31782.

Wongtrakul, J., Sukittikul, S., Saisawang, C., & Ketterman, A. J. (2012). Mitogen-activated protein kinase p38b interaction with delta class glutathione transferases from the fruit fly, *Drosophila melanogaster*. *Journal of Insect Science*, *12*(1). doi: 10.673/031.012.10701.

Wood, T. K. (2008). Molecular approaches in bioremediation. *Current Opinion in Biotechnology*, *19*, 572-578.

Zablotowicz, R. M., Hoagland, R. E., Locke, M. A., & Hickey, W. J. (1995). Glutathione s transferase activity and metabolism of glutathione conjugates by rhizosphere bacteria. *Applied and Environmental Microbiology*, *61*(3), 1054-1060.

Ziglari, T., & Allameh, A. (2013). The significance of glutathione conjugation in aflatoxin metabolism. *Chapter 13*. Retrieved on September 23, 2019 http://cdn.intechopen.com/pdfs/41614/InTech-The_significance_of_glutathione_conjugation_in_aflatoxin_metabolism.pdf.